Upper flow regime bedform stability

Cyclic steps, their geometry and position in a bedform stability diagram

By Joost Mulder, January 2010.

Department of Geo Sciences, Utrecht University, The Netherlands,
email: mulder.joost@gmail.com

Author:
Joost Mulder

Supervision:
Dr. George Postma
Matthieu Cartigny

Utrecht University
January 2010

Preface

As part of my study for the degree of Master of Science in Geology at the Faculty of Earth Sciences at the University of Utrecht, The Netherlands, I did a 6-month study at Eurotank Laboratories.

The study involved experimental work in a large tilting flume designed to model bedforms. The research was specifically on upper flow regime bed-forms, the so-called cyclic steps, their geometry and position in a bedform stability diagram.

This project gave me the opportunity to gain experience in doing empirical sedimentary laboratory research and gain knowledge about upper flow regime bedforms and their flow behavior. The research is complimented with four months of field research on turbidite systems in the Tabernas Basin in SE Spain and with a three months research on turbidites offshore Suriname at Petroleum Contracts, a division of Staatsolie Suriname N.V.

For the success of this project, I would like to thank the following persons:

- Dr. George Postma for his supervision, feedback on my thesis and the discussions we had that gave new insights.
- Dr. Janrik van den Berg, for his discussions that gave new ideas.
- Matthieu Cartigny for his dedicated role as a mentor, his stimulating discussions and critical comments that gave new ideas and insights.
- Thony van der Gon Netscher for supplying me with equipment and materials.
- Jeffrey Walet, classmate and colleague at Eurotank Laboratories, for his help with the experiments and the discussions that gave new insights.
- João Trabucho Alexandre, Jan de Vries and Jochem Bijkerk, for their help with experiments.

It has been an enormous pleasure and challenge for me to do this research project. I hope and wish that it adds insights and practical value for further experiments on upper flow regime bedforms and that the readers will enjoy it, as much as I enjoyed researching and writing it.

Utrecht, The Netherlands,
December 2009.

Abstract

Cyclic steps are upstream migrating bedforms of the upper flow regime, associated with slopes. They are characterized by trains of hydraulic jumps. Upstream of the hydraulic jump the flow is supercritical and the bed erodes, while downstream of the hydraulic jump the flow is subcritical and deposition takes place, resulting in an upstream migration of the bedform and the hydraulic jump. The formation of cyclic steps is empirically researched doing experiments using a tilting flume. Chute and Pools are described by Fukuaka et al. as a limiting case of cyclic steps for which the steepest bed slope realized just upstream of the hydraulic jump is still rather mild. Here, the definition of cyclic steps is discussed and a suggestion is made to use the term cyclic steps with the additional information of the state of the hydraulic jump, which can be 'normal' or 'submerged'. The sensitivity of the cyclic step geometry is analyzed by the median sediment grain size and flow characteristics. The geometry of the cyclic step can be described by the length, the height, the slope and the position of the highest point. Per geometry characteristic the following parameters are tested: the flow specific discharge, the flow sediment volume concentration, the median sediment grain size, the average Froude number, the mobility parameter, the streampower, and the relative flow depth. This resulted in two functions using the streampower to obtain the cyclic step's length and height. Based on the experiments, a bedform stability diagram is created for the upper flow regime using streampower and slope to plot upper plane bed, antidunes, cyclic steps with a normal and with a submerged hydraulic jump.

Introduction

Bedforms in the upper flow regime are related to supercritical flow, which can be described by the Froude number (Formula 1), where h denotes flow depth, U denotes depth averaged flow velocity and g denotes the gravitational acceleration. When "$Fr < 1$" the flow is called subcritical, "$Fr = 1$" critical and "$Fr > 1$" supercritical.

$$Fr = \frac{U}{\sqrt{gh}} \tag{1}$$

Cyclic steps are a bedform associated with slopes and created by a flow that repetitively alternates from sub- to supercritical. A hydraulic jump occurs at the transition from super- to subcritical flow. The cyclic steps aggrade at the stoss side, where the local bed slope dips upstream, and erode at the lee side, where the local bed slope dips downstream. This results in an upstream migration of the bedform (Taki & Parker, 2005; Cartigny et al., 2009).

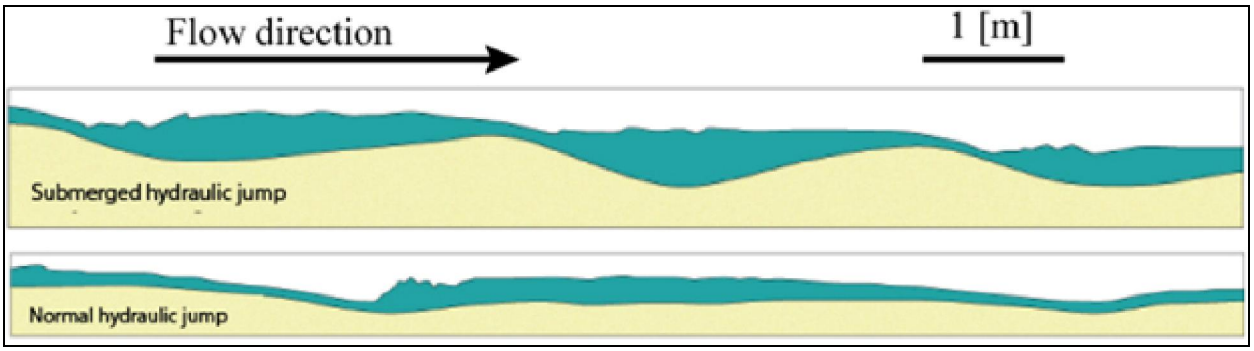

<Figure 1.1, Cyclic steps with a submerged and a normal hydraulic jump. The flow is from left to right. The drawings are directly traced from the video images. (modified after Cartigny et al.,2009).>

Cyclic steps have been observed in the field and described by Winterwerp et al. (1992) and Mastbergen (1989). Taki & Parker (2005) did flume experiments on sub-aerial cyclic steps to describe and quantify the processes involved. Spinewine et al., (2009) produced sub-aqueous cyclic steps using a salt dilution and observed and quantified their formation. Cyclic steps are explained theoretically by Mastbergen (1989), Parker & Izumi (2000), Fagherazzi (2003) and Sun and Parker (2005). Cyclic steps can form under conditions of bed aggradation and degradation and can migrate up dip when in equilibrium. The migration of cyclic steps produces backsets as the remnants of the hydraulic jump. Backsets have been interpreted in ancient deposits of rivers (Power, 1961; Fralick, 1999), fan deltas (Nemec, 1990; Massari, 1996) and volcanic base surges (Schmincke, et al. 1973). Cartigny et al. (2009) gives a process-based description of the upper flow regime bedforms. The relation for upper flow regime bedforms has not yet been quantified.

Thanks to multibeam surveys, more cyclic steps are recognized in subaqueous canyons, and interpreted as a bedfrom created by turbidity currents (Fildani et al., 2006). Two surveyed canyons are the Monterrey canyon (Schmidt et al., 2005) and Eel canyon (Lamb et al, 2008), both offshore California, showing large sets of cyclic steps.

Alternative names for cyclic steps are sediment waves and chute and pools. The chute and pool morphology is described as a limiting case of cyclic steps for which the steepest bed slope realized just upstream of the hydraulic jump is still rather mild (Fukuoka et al., 1982, in Taki & Parker, 2005). The term cyclic steps is used for the entire class of spatially periodic bedforms, where each wavelength is delineated by an upstream and downstream hydraulic jump (Taki & Parker, 2005). Another definition links the terms chute and pool and cyclic step to flow behavior (Cartigny et al., 2009), using the state of the hydraulic jump, which can be normal or submerged (figure 1.1). They relate chute and pools to the normal and cyclic steps to the submerged hydraulic jump. The mentioned definitions for cyclic steps give a problem when the bedform is to be described from the geological record, where the state of the hydraulic jump cannot be observed and the steepest bed slope realized just upstream of the hydraulic jump cannot be quantified by a suggestive term as being rather mild. The usability in the geological record for the definition of cyclic steps would be improved if the term "rather mild" is quantified.

The cyclic step geometry can simply be described by an inclined triangle, using the base length (l_s), the height (h_s) the location of the highest point (x_s) and the regional slope (i_r) of the cyclic step (figure 1.2).

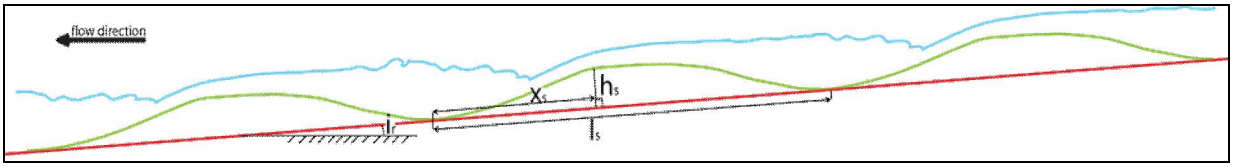

<Figure 1.2, A train of three cyclic steps is drawn. The bed surface is indicated with a green line, the water surface is in blue and the regional slope is drawn in red. The regional slope has an angle "i". The length of a cyclic step "l_s" is defined as the distance between troughs parallel to the regional slope. The highest point of a cyclic step "h_s" is defined perpendicular to the regional slope with a location "x_s" defined as the distance from the downstream trough parallel to the regional slope. The flow direction is from right to left.>

Relations between bedforms and flow parameters are plotted in bedform stability diagrams. Proven bedform stability diagrams are:

- Simons & Richardson (1961): using dimensionless hydraulic parameter versus particle shear Reynolds number.
- Bonnefille-Pernecker (1963): using Bonnefille dimensionless particle diameter versus Reynolds number.
- Simons and Richardson (1966): using streampower versus median sediment grain size
- Simons & Richardson (1966): using streampower versus median fall diameter.
- Vanoni (1974): using Froude number versus relative flow depth.
- Van Rijn (1984): using transport stage parameter versus median sediment grain size.

- Boguchwal & Southard (1990): using flow velocity versus median grain size.
- Van den Berg & Van Gelder (1993): using mobility parameter versus grain size.

Next to the lower flow regime bedforms, they cover upper plane bed and antidunes from the upper flow regime. Cyclic steps seem to be a stable bedform, but are not included. The proven stability diagrams provide the parameters that need to be quantified in my study. The physical behavior of the flow and/or bed can be described by the following parameters:

- Flow specific discharge q [m2/s] (product of flow velocity U [m/s] and flow depth h [m]);
- Median sediment grain size D_{50} [m];
- Streampower P [-];
- Froude number Fr [-];
- Mobility parameter θ [-];
- Relative flow depth h/D50 [-];
- Flow Sediment volume concentration c [%];
- Step geometry h_s/l_s [-].

Once quantified, relations between flow and bed characteristics can be drawn to meet the objectives, which are in threefold:

- Relate flow characteristics to the cyclic step geometry, so that palaeoflow conditions can be determined from deposits.
- Sharpen the definition of cyclic steps by quantifying the local or regional slope that distinguishes between deposits associated with a normal and a submerged hydraulic jump.
- Configure a bedform stability diagram that includes cyclic steps.

The data used to meet the objectives is gathered doing flume experiments. The flume configuration did not have possibilities to measure the discharge using sensors or other electronic equipment. Therefore, a study had to be done to visually determine the flow velocity using tracers. This resulted in a formula for the Froude number on the highest point of a cyclic step, with the slope as a variable. The velocity and specific discharge could be calculated using the Froude number (formula 1). This sub-study is a very important part of the thesis and belongs to the methodology used to meet the three objectives. Because this part became very important, it will is described in paragraph “Research to the Froude number on the highest point of a cyclic step” of the “Results” chapter.

Notation

Parameters:

Fr = Froude number

Fr_h = Froude number on the highest point of a step

U, v = flow velocity

g = acceleration of gravity

h = flow depth, perpendicular to the local slope.

x_s = distance between highest point of a step and the downstream trough, parallel to the regional slope

l_s = step length, measured from trough to trough

h_s = step height, perpendicular to the regional slope, with the line from trough to through as base.

i_r = regional slope

q = flow specific discharge

D50, D_{50} = median sediment grain size

P = streampower

θ' = effective shields parameter or mobility parameter

c = flow sediment concentration

X-f, x-feed = sediment feeder input setting

P = mixture density

ρ_s = sediment density

ρ_w = water density

f = chezy friction coefficient

R^2 = the correctness of a function, with 1 as a 100% fit.

Bedforms:

5, PB = upper plane bed

7, AD = antidunes

8, CS = cyclic steps (chute pool)

Methodology

Data for upper flow regime bedforms was needed to work towards the three objectives. The data is produced doing flume experiments in the Eurotank Laboratories at the Utrecht University. This chapter will explain the equipment and methods used to measure and calculate the variables. The research on the Froude number on the highest point of a step, which is not an objective of this study, but an important research part of the methodology to work towards the objectives, will be handled in the results section, paragraph “Research to the Froude number on the highest point of a cyclic step”.

The flume

The flume has a total length of 12 meter and a total width of 0.48 meter. The flume can be tilted from 0 to 4 degrees. In order to suppress three dimensional effects and to minimize the amount of sediment needed for an experiment, a construction was made with a length of 6 meter and a width of 0.05 meter. A 0.2 meter high weir was positioned upstream of the flume to regulate the water discharge and to make it possible for the bed to build its own equilibrium slope, as illustrated in a schematic drawing (figure 2.1).

To develop stable bedforms, the sediment infow has to be equal to the sediment outflow. The pump, which is integrated into the flume, can set the water inflow, but not the sediment inflow. Therefore, a sediment feeder is used to introduce sediment 0.5 meter from the upstream end into the flow. Just downstream of the weir, a pool is created to buffer the upstream migrating bedforms. Downstream of the flume a weir with a height of 0.08 meter makes that the downstream end of the bed remains at the same level. The events are recorded by cameras for later observations and measurements.

Logging

The bedforms created are recorded using two industrial cameras (Basler Pilot and Basler Scout) combined with a computer using video capture software called “streampix 4”. The total recorded image of the flume is 2.6 meters wide, positioned from 1 to 3.6 meter from the upstream weir. After recording an event, the video images can be viewed as a movie for observation of the processes or per timeframe for measurements in space and time. The Software used for measuring distances is called “MB-Ruler 3.5”. Calculation and measure methods for specific tasks are explained later in this chapter.

Run conditions

Before each run an initial bed was made. Wet sediment is put into the flume using a shovel. Water is injected into the bed using a garden-hose. Quickly drilling the needle of the garden-hose into the bed up to the flume floor removes the air bubbles in the sand. Care is taken to repeatedly drill every part of the bed with same force and duration until no bubbles are visible along the flume window anymore. To rule out porosity differences in the initial bed and the bed created by the bedforms, the porosity is tested several times. The tests gave a porosity of 40 ± 2 % for both the bed formed by sub- and supercritical flow and the drilled initial bed.

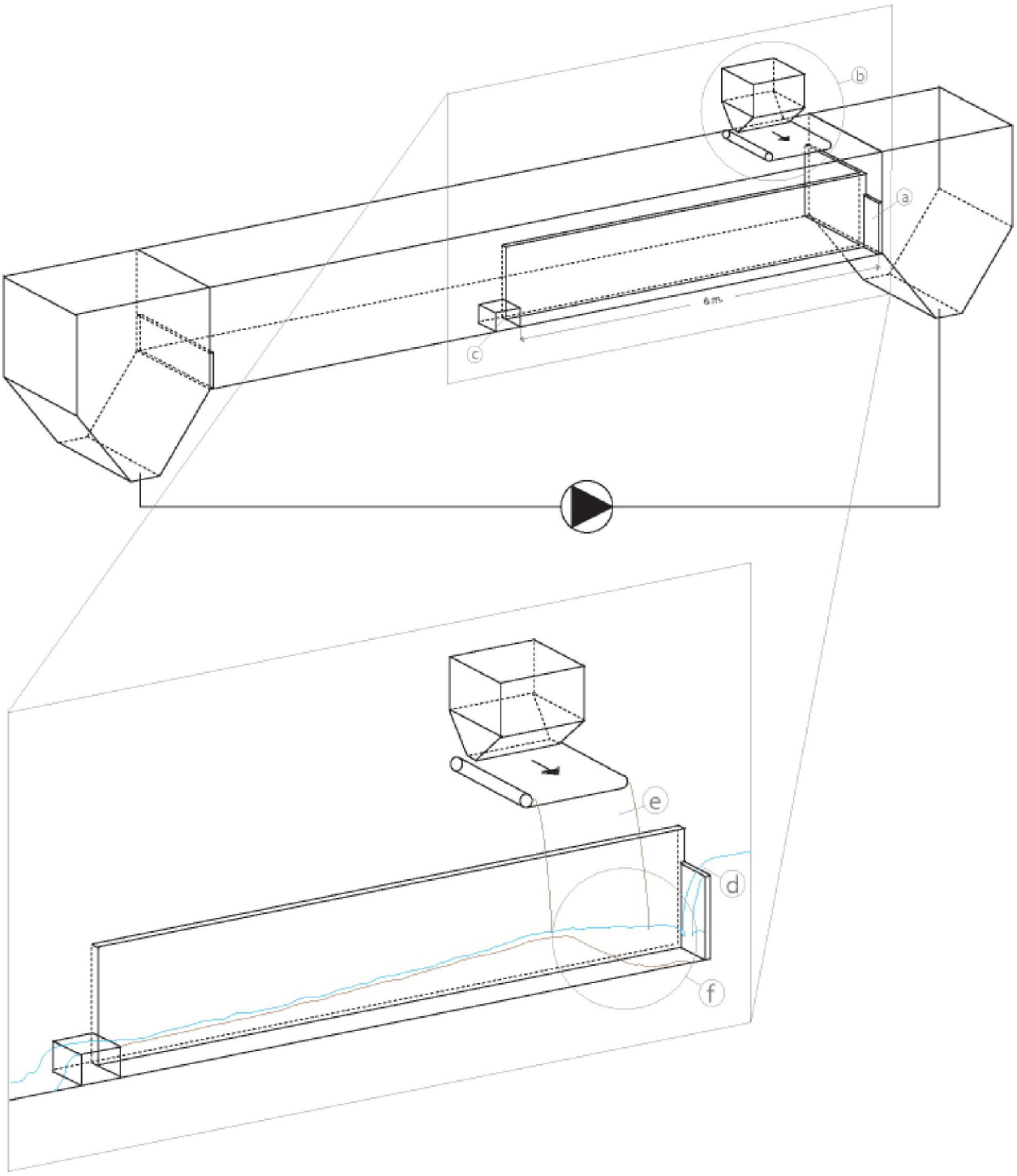

<Figure 2.1: Schematic flume configuration. A schematic representation of a flume experiment, with the flowing water, the sediment inflow and the bed are drawn in the zoomed part of the actual flume in a 2 dimensional way. (a) Upstream weir. (b) Sediment feeder. (c) Downstream wall. (d) Water inflow. (e) Sediment inflow. (f) Pool. (modified after Cartigny et al., 2009)>

A run starts with an initial slope and water discharge. The water flow starts transporting the sediment immediately and alters the slope. To create a stable bed with a constant slope over time, the inflow of sediment has to be the same as the outflow. Therefore a sediment feeder was installed. A bedform is assumed stable when the slope and length of the bedform structures do not change during a period of one minute. The variables in this set up are the slope and the water discharge. By varying these, the related sediment discharge had to be found to get stable bedforms.

A difficulty in this set up is that the pool (figure 2.1 f) has a natural weir created by the bed. The sediment inflow has to be the same as the sediment outflow, meaning that the bed had to stay at the same level. With a marker pencil a stripe is drawn on the window of the flume where the initial bed is leveled. The discharge pump is turned on and the pool (figure 2.1 f) starts to fill. Once it overflows, grains will be picked up by the flow and degrade the bed. The sediment feeder has to be set manually to counter the degradation and give the flow a sediment concentration for the bed to be in equilibrium. It may take a minute to tune the sediment feeder for the bed to stay at the level of the stripe drawn on the flume window. Once equilibrium exists for a period of one minute, the experiment is successful.

Within one minute several cyclic steps have had time to migrate into the upstream pool. One minute is long enough to mark a run as stable. In an unstable situation, where sediment inflow is not equal to the outflow, the bed would aggrade or degrade with accelerating speed. This alters the natural weir of the pool (figure 2.1 f), which alters the flows discharge. An altered flow discharge only strengthens the effect of bed aggradation or degradation and can easily be noticed with the naked eye.

Sediment concentration

The sediment concentration is simply calculated using the discharge of the sediment feeder divided by the sum of the flow and sediment discharge. Before this calculation can be made, the sediment discharge needs to be determined.

The used sediment feeder has an analog button with values from 0 to 9 with a precision of 0.05. A sediment discharge chart (figure 2.2) is made relating the input value of the sediment feeder to specific sediment discharge. This is done by turning on the sediment feeder for a certain time. The sediment flowing out of the feeder is collected in a basket. The volume of the collected sand is measured and corrected for the porosity, which is 40%. The corrected volume is divided by the run time of the feeder, and notated in m^2/s, which is the specific discharge. These measurement are done three times per sediment input value and averaged (Table 2.1, A, B & C), to create the sediment feeder discharge chart. This process is repeated for all sediment (i.e. for the 320, 185 and 112 µm sediments). While doing a run, the sediment feeder value and time are notated when changed. The exact sediment discharge can be read from the graph afterwards.

(A) Sediment feeder - 320 µm

X-f	a	b	c	st.dev.	std.err.	AVG [ml/s]	[l/s]	porosity corr.	q [m2/s]	std.err.
1	38	37	32	3.21455	1.86	36	0.036	0.021	0.000428	2.227E-05
1.5	180	185	190	5	2.89	185	0.185	0.111	0.002220	3.464E-05
2	300	300	325	14.43376	8.33	308	0.308	0.185	0.003700	0.0001
2.5	370	370	370	0	0.00	370	0.370	0.222	0.004440	0
3	450	510	460	32.1455	18.56	473	0.473	0.284	0.005680	0.0002227
4	570	600	490	56.86241	32.83	553	0.553	0.332	0.006640	0.000394
5	710	730	700	15.27525	8.82	713	0.713	0.428	0.008560	0.0001058
6	900	750	755	85.19585	49.19	802	0.802	0.481	0.009620	0.0005903

(B) Sediment feeder - 185 µm

X-f	a	b	c	st.dev.	std.err.	AVG [ml/s]	[l/s]	porosity corr.	q [m2/s]	std.err.
0.7	10	4	6	3.05505	1.76	7	0.007	0.004	0.000080	2.117E-05
0.8	18	18	18	0	0.00	18	0.018	0.011	0.000216	0
0.9	25	20	20	2.886751	1.67	22	0.022	0.013	0.000260	0.00002
1	35	33	32	1.527525	0.88	33	0.033	0.020	0.000400	1.058E-05
1.2	50	57	57	4.041452	2.33	55	0.055	0.033	0.000656	2.8E-05
1.5	65	68	66	1.527525	0.88	66	0.066	0.040	0.000796	1.058E-05
2	85	91	92	3.785939	2.19	89	0.089	0.054	0.001072	2.623E-05
4	100	96	98	2	1.15	98	0.098	0.059	0.001176	1.386E-05

(C) Sediment feeder - 112 µm

X-f	a	b	c	st.dev.	std.err.	AVG [ml/s]	[l/s]	porosity corr.	q [m2/s]	std.err.
0.7	2	4	3	1	0.58	3	0.003	0.002	0.000036	6.928E-06
0.8	13	9	10	2.081666	1.20	11	0.011	0.006	0.000128	1.442E-05
0.9	27	19	26	4.358899	2.52	24	0.024	0.014	0.000288	3.02E-05
1	30	33	35	2.516611	1.45	33	0.033	0.020	0.000392	1.744E-05
1.2	45	44	43	1	0.58	44	0.044	0.026	0.000528	6.928E-06
1.5	60	62	63	1.527525	0.88	62	0.062	0.037	0.000740	1.058E-05
2	79	80	81	1	0.58	80	0.080	0.048	0.000960	6.928E-06
4	90	90	91	0.57735	0.33	90	0.090	0.054	0.001084	4E-06

<Table 2.1 A-C: Per sand three measurements are done per sediment feeder input setting, giving the specific discharge. X-f is the sediment feeder input value. a, b and c are the three measurements. AVG is the averaged uncorrected discharge. q is the specific discharge corrected for the porosity.>

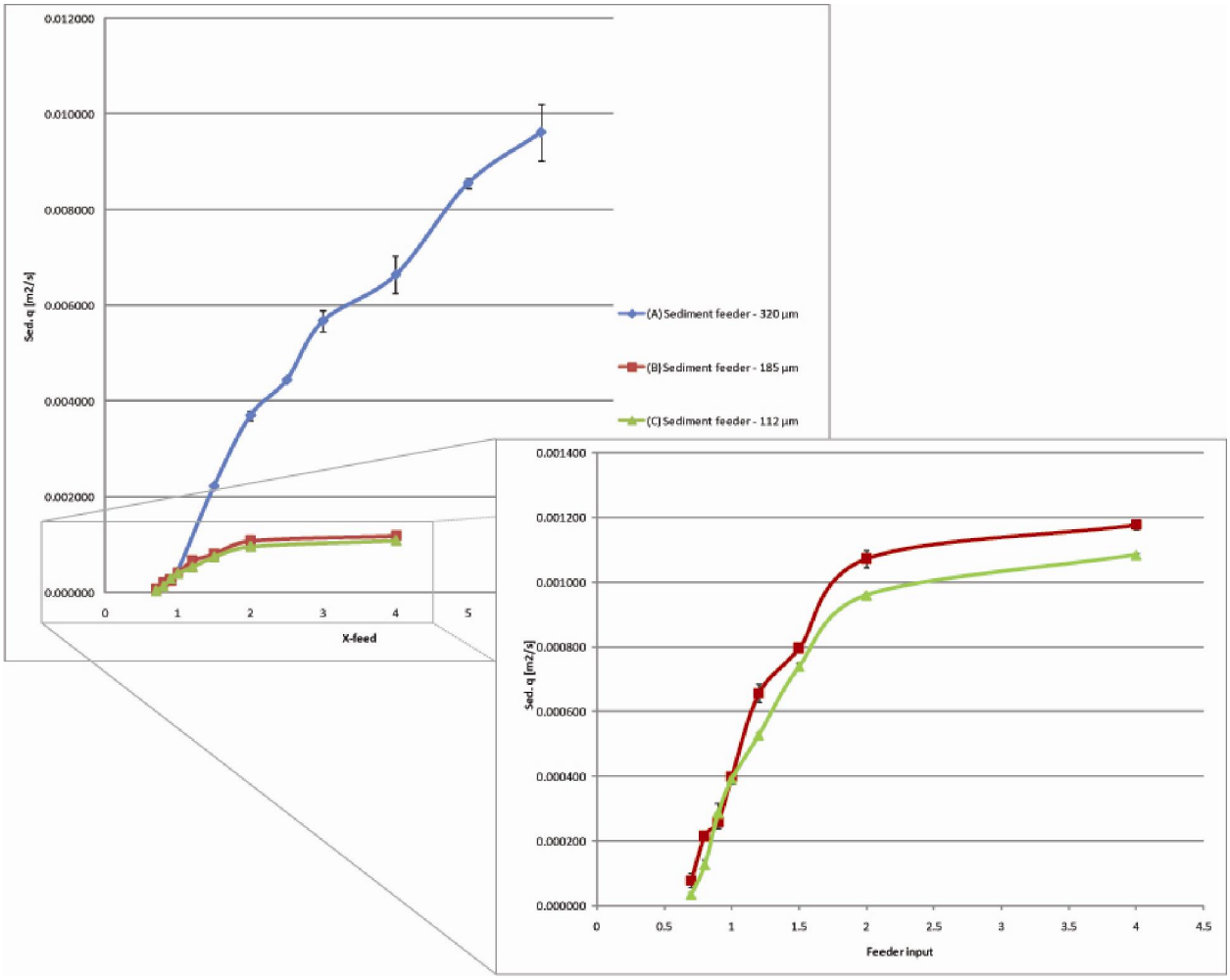

<Figure 2.2, Sediment feeder discharge chart.>

Regional slope

The regional slope 'i_r' is measured by using the logged image of the two cameras. The flume slope, which is logged per run, serves as reference. The software tool "MB-Ruler" is used to measure the regional slope of the bed. This could be done in two ways, which both gave the same results.

The first way is to set the x-axis of the software tool parallel to the flume slope. With this reference, the angle is simply measured between the most downstream and most upstream troughs of one image, which has a maximum width of 1.8 meter. This angle plus the flume slope angle is the regional slope.

The second way also uses the most downstream and most upstream troughs between two Images, which has a maximum width of 2.6 meter (figure 2.3), and the flume slope as reference. The software tool is set on right coordinates by using the ruler, which is taped on the flume, as reference. By measuring the change of elevation of the troughs divided by their horizontal spacing from each other gives the slope. This slope plus the flume slope gives the regional slope of the bed.

It does not matter for the results which way to use. The first way is the easiest and fastest way to determine the slope and is used more often.

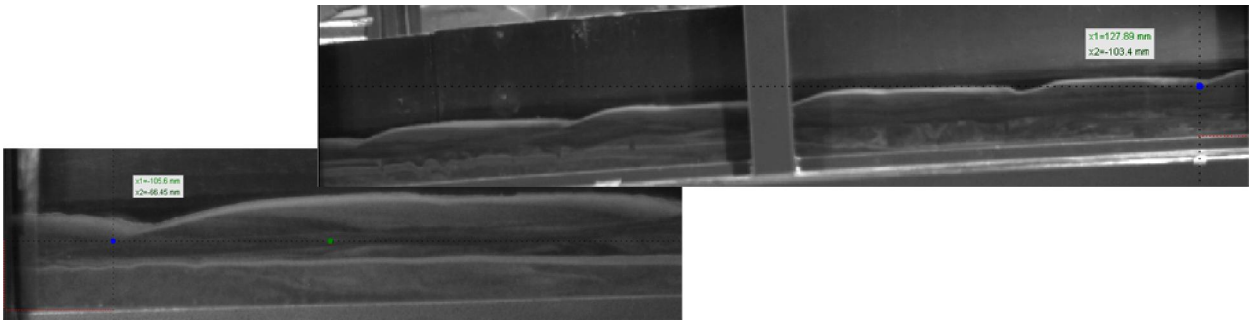

<Figure 2.3, The two camera images from run 57, 6:02.362. The positions of the most outer troughs on the image are measured with the flume as reference. Their change in elevation over vertical distance gives the slope with respect to the flume slope.>

Step height and length

The step length is the distance of one step, measured from trough to trough. The step height is the distance from the troughs to the highest point of the step, measured perpendicular to the overall bed slope. Both lengths are determined with the screen measuring tool. Figure 2.4 shows how the distances are measured using the software measuring tool of the program 'MB-ruler'.

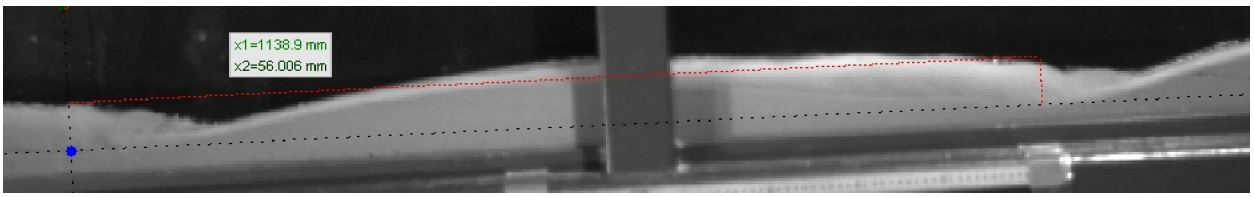

<Figure 2.4, Measuring the length and height of a step at run 44, 7:34.674. The reference line is set, so it cuts straight through the troughs. The height is measured perpendicular to this.>

Bedform definitions

The bedform is called plane bed, if a near-horizontal surface develops, characterized by primary current lineation on the sediment surface. The bedform is called antidunes if a periodic sinuous bed forms develops, which can be migrating up- or downstream or stay focused, which is also called standing-waves. The definition for cyclic steps used, is for the entire class of spatially periodic bedforms, where each bedform is delineated by an upstream and downstream hydraulic jump, of which the process creating these bedforms is already described in the Introduction of this thesis. Later, in the results and interpretation section, the definitions for cyclic steps are discussed.

Average flow depth

The average flow depth is measured by taking the average of ten flow depth measurements distributed along one bedform step. The measurements are done perpendicular to the bed (figure 2.5).

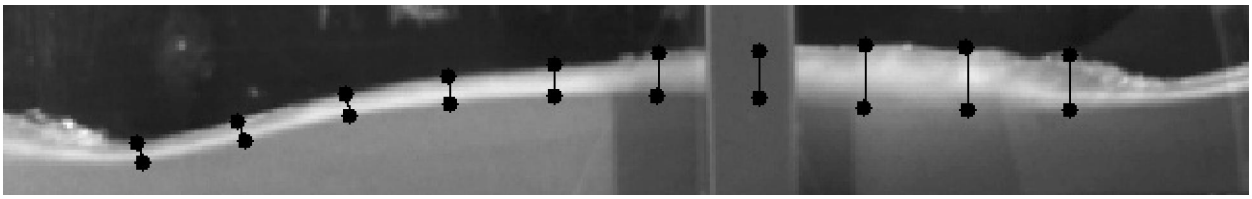

<figure 2.5, The average flow depth of one cyclic step (run 29, 4:10.190) is determined by taking the average of measurements done on a grid of ten points per step.>

Effective shields parameter

A parameter to be used to meet the second goal "to configure a bedform stability diagram that includes cyclic steps" is the mobility parameter, also known as the effective shields parameter (formula 4).

$$\theta' = \frac{U^2}{g(\rho_s - \rho_w)D_{50} f^2} \tag{4}$$

Where D_{50} denotes the median sediment grain size, ρ_s denotes the sediment density and ρ_w denotes water density. The following values are used:

$$\rho_s - \rho_w = 1.65$$

$$g = 9.81$$

The mobility parameter uses the Chézy friction coefficient shown in formula 5, which is related to the grains and not to the bedforms present.

$$f = 18\log\left(\frac{4h}{2.5D_{50}}\right) \tag{5}$$

Streampower

The streampower is proven to be the dominant factor for the sediment transport rate in natural rivers and flumes (Yang & Stall, 1974) and might therefore be a good parameter to relate upper flow regime bedforms with, where sediment transport is relatively high. The streampower can be derived using a momentum balance (Van Rijn, 1993; formula 6). This parameter is successfully used by Simons & Richardson (1966) in a bedform stability diagram.

$$\mathrm{P} = gihU\rho \tag{6}$$

Sediment

The sediment consists of silica sand with a density of 2650 kg/m^3. The grain size is an average of three measurements done by laser diffraction and shown in table 2.2.

	Sand 1	Sand 2	Sand 3
D10	186	122.83	52.8933
D50	312.333	184.47	118.657
D90	499.667	274.943	217.017
St.Dev.	128	64.002	70.023

<Table 2.2. The properties of the three used sediments. The sizes are averages of three measurements that are also used to calculate the standard deviation.>

Results

The flume experiments

In total 57 runs have been conducted and logged. During the runs different settings for slope and discharge have been empirically tested, using the three kinds of sediment. Sand A (320 µm) is used for runs 1 to 32, sand B (185 µm) is used for runs 33 to 45 and sand C (112 µm) is used for runs 46 to 57. In the flume logbook, the sediment feeder settings are logged. Every time the feeder settings changed during a run, time and sediment feeder settings were notated. In total 39 out of the 57 runs have been selected for analyses and are shown in Table 3.1. The runs that were not selected do not show the required stability of bedforms.

Bedform	Run	D50 (m)	h @ highest point	AVG v [m/s]	AVG h/step	Step height	step Length	Slope Degrees	X-feed	sed.q	std.err. Sed.q
CS	21	0.00032	0.023	0.017		68	530	6	0.9	0.000252	1.114E-06
CS	22	0.00032	0.022	0.016		75	544	6	0.8	0.000216	1.114E-06
CS	22	0.00032	0.022	0.019		68	490	6.5	0.9	0.000252	1.114E-06
CS	23	0.00032	0.045	0.030		90	820	4	0.9	0.000252	1.114E-06
CS	23	0.00032	0.045	0.032		97	876	4.3	0.9	0.000252	1.114E-06
CS	29	0.00032	0.058	0.038		80	957	1.6	0.85	0.00023	1.114E-06
CS	34	0.000185	0.037		0.033	55	750	2.1	0.9	0.00026	0.000001
CS	34	0.000185	0.040		0.033	54	770	2.1	0.95	0.00034	0.000003
CS	43	0.000185	0.049	0.90	0.055	75	1200	1.1	2	0.001072	1.311E-06
CS	43	0.000185	0.095		0.074	75	3000	1.1	5	0.0012	6.928E-07
CS	44	0.000185	0.018		0.013	28	365	3.4	0.9	0.00026	0.000001
CS	44	0.000185	0.050		0.034	43	910	3.4	1.1	0.000392	9.00E-07
CS	44	0.000185	0.050	0.58	0.034	43	910	3.4	1.1	0.000800	9.00E-07
CS	44	0.000185	0.034	0.56	0.024	98	1200	3.4	1.1	0.000200	9.00E-07
CS	49	0.000118		0.83	0.035	40	1400	0.8	1	0.000288	8.718E-07
CS	49	0.000118	0.085	0.95	0.078	30	2500	0.8	1.6	0.000128	5.292E-07
CS	50	0.000118	0.025	0.52	0.019	31	845	1	0.85	0.000128	1.00E-06
CS	51	0.000118	0.022	0.40	0.022	36	800	1.4	0.9	0.000288	1.51E-06
CS	51	0.000118	0.025	0.43	0.028	38	840	1.4	0.8	0.000288	7.211E-07
CS	51	0.000118	0.050	1.43		60	1800	1.4	0.8	0.000128	7.211E-07
CS	52	0.000118	0.023	0.51	0.021	53	700	1.6	0.9	0.000128	1.51E-06
CS	53	0.000118	0.021	0.44	0.021	40	600	2	0.9	0.000128	1.51E-06
CS	53	0.000118	0.019	0.36	0.023	46	705	2	0.8	0.000288	7.211E-07
CS	54	0.000118	0.023	0.45	0.023	37	610	2.5	0.8	0.000288	7.211E-07
CS	55	0.000118	0.021	0.38	0.023	59	628	3.1	0.9	0.000128	1.51E-06
CS	56	0.000118	0.010	0.34	0.013	26	430	1.6	0.8	0.000528	7.211E-07
CS	56	0.000118	0.030	0.51	0.025	73	816	1.7	1.2	0.000080	3.464E-07
CS	57	0.000118	0.008		0.010	35	600	3.1	0.75	0	6.00E-07

CS	57	0.000118	0.004		0.004	42	484	3.7	0.75	0.000216	6.00E-07
CS	57	0.000118	0.012		0.010	82	961	4.5	1	0.00008	8.718E-07
CS	57	0.000118	0.030		0.035	109	967	3.5	1	0.000216	8.718E-07
FB	42	0.000185	0.010		0.011			0.5	0	0.000216	0
FB	50	0.000118		0.76	0.040			1	1	0.000288	8.718E-07
AD	28	0.00032	0.042		0.038	13	350	1	0.8	0.000200	1.114E-06
AD	42	0.000185		0.54	0.014	5	110	0.5	0.7	0.000252	1.058E-06
AD	42	0.000185		0.63	0.030	5	350	0.5	0.8	0.000216	0
AD	42	0.000185		0.68	0.022	5	350	0.5	0.8	0.000252	0
AD	47	0.000118		0.55	0.013			0.25	0.9	0.000252	1.51E-06
AD	48	0.000118		0.73	0.018			0.25	0.85	0.000252	1.00E-06

<Table 3.1, The table shows the measured data that could be used. They are sorted on bedform type. The Run number, the median grain size 'D50', the flow depth at the highest point 'h', the average speed AVG v', the average flow depth along a step 'AVG h/step', the step height, the step length, the slope, the sediment feeder setting 'x-feed', the sediment specific discharge 'sed q' and the standard error on the sediment discharge 'std.err. Sed.q' are given.>

Pilot runs to configure the flume set up

The first two runs were performed with a total flume width of 0.42 m and the maximum slope of the flume, which is 4°. No sediment feeder was used yet, only an initial bed was made. No upper flow regime bedforms could be produced in this flume configuration and channels, which is a 3d effect, formed at the start of the run, when the discharge was still low. Because Taki & Parker (2005) produced cyclic steps on slopes larger than 10 degrees, the assumption was made that the slope was too low to produce supercritical bedforms. In order to experiment with larger slopes, a new flume configuration was constructed. At the same time, the flume was made narrower, to remove the 3d effects of the flow and bedforms. The flume section, as described in chapter methodology, was created.

In the next pilot runs (3 to 7) different settings with slope and discharge were tested on a high slope (4° to 12°). The effect of erosional cyclic steps could be observed, but no stable bedform could be created. This was the result of erosion that started at the upstream end of the bed. To counter erosion and create a stable bed with a constant slope, sediment had to be added during the runs. Therefore, a sediment feeder was installed in run 8. A solution had to be found to measure the concentration of the sediment in the flow. With the new sediment feeder, this problem was solved too. The sediment discharge of the feeder could be used to calculate the concentration of sediment in the flow under equilibrium conditions ($q_{in} = q_{out}$), as described in the methodology chapter. The new installed sediment feeder could not supply the relatively high sediment discharge needed for the flow. The sediment feeder was adjusted for run 9, to supply a larger sediment discharge. Even with the larger sediment discharge there was too much erosion and no stable bedform could develop.

The next runs, 10 to 20, different settings were tried, which resulted in unstable bedforms. For run 10 and 11 the slope was decreased to 3.9°, resulting in a run with cyclic steps that were not stable. They were formed at the end of the three meter long flume, for just a few seconds for both runs. From run 12

on, the flume was extended to a total length of 6 meter, to better observe the continuum of bedform morphologies. Run 12, 13 and 14 shows cyclic steps that are not stable and eroded to the floor of the flume. After run 12, no dry sediment was left to feed the sediment feeder. From now on sediment had to be dried in an oven. Run 13 went wrong because the sediment in the feeder was still a bit wet and it jammed. In run 14, no initial bed was made. A trial run was done to let the flow accumulate sediment. It turned out that the floor of the flume was to smooth for the sediment to settle. Run 15 to 20 show cyclic steps with a bit fluctuating discharge, due to difficulties setting the right conditions for both the flume pump and sediment feeder. It turned out that both machines have to turn for at least one minute, before they run with a stable discharge.

Runs used for the data matrix

Run 21 to 23 show the first useful cyclic steps. The next step was to produce antidunes and flat bed, to compare settings with and to relate them with known bedform stability diagrams.

During the next runs, 24 to 30, attempts are given to find criteria for the formation of flat bed and antidunes. Run 24 is a try to produce antidunes on a slope of 1°, which appeared to be too high and the flow was erosional. Run 25 produced a flat bed for just a few seconds, before the sediment feeder jammed the pathway of the flow with too much sediment. Runs 26 and 27 show flat bed and antidunes, but with a slightly fluctuating discharge. Again, it appears difficult to hold the beginning of the bed at the same height by adjusting the sediment feeder to the flow discharge. From run 27 on, a new lens is set on to one camera, which could record a larger angle. Run 28 is the first stable run with antidunes that could be used for measurements. During this run antidunes were conducted on a slope of 0.1°. Run 29 shows stable cyclic steps and run 30 shows flat bed and antidunes. The bedforms conducted during run 30 are a bit unstable, because of a slightly changing bedslope, as a result of a slightly changing flow discharge.

Another two tries (run 31 and 32) with the current sand are given to produce cyclic steps. Run 31 shows cyclic steps, but the run was too short to form a stable bedform. This was due to a sediment feeder that ran empty. Run 32 shows unstable cyclic steps, because of difficulties setting the flume pump and sediment feeder at right values.

In the next runs (34 to 44), sand A (320 µm) is replaced by sand B (185 µm) which is expected to be more stable in producing cyclic steps. Due to dilatancy water must flow into the bed when grains are eroded and a hydraulic gradient is present (Van Rhee, 2007). This hydraulic gradient pushes the top layer of grains on the bed and will hinder erosion. This gradient will increase with the erosion velocity and decrease with the permeability. The permeability of a bed decreases when the grain size becomes smaller (Shepherd, 1989). It is therefore expected that the 185 µm sand has larger erosion resistance and is therefore more stable to produce supercritical bedforms at slopes.

During run 33 there were problems with the sediment feeder, since it was too sensitive to set with the new sand. The problem was fixed in run 34 which shows cyclic steps. The opening of the sediment feeder is made smaller for this run. Run 35 produced cyclic steps that were too long to measure. Runs 36 to 39 failed, because to flume was leaking sediment from beneath. This was caused by a rubber strip

that was damaged between the main flume and the smaller build flume section. Run 40 shows cyclic steps that were unstable, because a few times an antidune appeared between two steps. Run 41 shows a combination of cyclic steps, antidunes and flat bed.

In the next two runs (42 and 43) the point were antidunes or flatbed evolve to cyclic steps is searched for and a tracer is introduced to visually determine the flow velocity on the recorded images for later usage in determining the Froude number on the highest point (paragraph "Research to the Froude number on the highest point of a cyclic step"). The tracer used is dissolved potassium permanganate, of which 0.01 liter is poured at once at the downstream end of the pool (Figure 2.1 f), to create a well visible purple cloud in the flow. Run 42 shows antidunes. During the run the discharge is changed allowing more different measurements to be made. Run 43 shows cyclic steps that attend to have smooth antidunes at their crest. It is not sure if the bedform can be called cyclic steps, antidunes or flat bed. Run 44 shows a bedform evolving from flatbed to antidunes to cyclic steps.

For the next runs (45 to 57) sand B (185 µm) is replaced by sand C (112 µm) and flat bed, antidunes and cyclic steps are produced. During runs 45 and 46, no stable bedform was present. Run 47 shows flat bed and antidunes. Run 48 shows flat bed, antidunes and cyclic steps, but all unstable. Run 49 to 51 and 53 to 57 show cyclic steps. More measurements can be taken from a run, as the discharge is changed during a run and a new stable bedform could evolve. The tracer at run 55 is hard to recognize because of poor illumination. Run 52 shows cyclic steps, but the run was too short to produce a stable beform. The steps vary in length and sometimes show an antidune between two steps.

Research to the Froude number on the highest point of a cyclic step

The available flow velocity meters appeared too big to be used in the present set up. Therefore, we used the Froude number (Formula 1) to obtain depth averaged flow velocity. This method required a point on the bedform where the Froude number is known (i.e. where Fr = 1).

A series of runs are conducted using a tracer to visually determine the flow velocity on the recorded images. These are runs 44, 48, 49, 51, 53, 54 and 56. The displacement of the tracer is measured per time step of 30 to 165 milliseconds, depending on the desired resolution (e.g. the tranquil flow, just downstream of a hydraulic jump does not show much acceleration, so steps of 165 milliseconds are sufficient, while just upstream of a hydraulic jump, the flow accelerates quickly and a higher resolution, in this case 30 milliseconds, is desired). This results in a velocity profile of the flow along the bed. To get the Froude number distribution along a cyclic step, the flow depth is measured and used together with the flow velocity in formula 1 to get the local Froude numbers (Table 3.2).

<Table 3.2 (next page), The Froude number distribution along a cyclic step is calculated by measuring the flow depth and the displacement per time segment. Depending on the desired resolution time segments of 30 to 165 ms are used. Per run the name, the time of the logged image when measuring for this data started, the step length and height are given. Time is in milliseconds, x and h in millimeters and v in meters per second.>

Run	44		length	865	mm
st. t.	6.48.870		heigth	68	mm
Time	X[mm]	x [%]	h[mm]	V[m/s]	Fr
48987	34	3.93	60		
49109	86	9.94	58	0.43	0.57
49206	122	14.10	57	0.37	0.50
49318	153	17.69	51	0.28	0.39
49445	195	22.54	48	0.33	0.48
49547	224	25.90	45	0.28	0.43
49669	266	30.75	42	0.34	0.54
49750	294	33.99	37	0.35	0.57
49852	324	37.46	35	0.29	0.50
49953	361	41.73	31	0.37	0.66
50019	387	44.74	29	0.39	0.74
50096	427	49.36	26	0.52	1.03
50177	477	55.14	24	0.62	1.27
50243	539	62.31	23	0.94	1.98
50309	598	69.13	20	0.89	2.02
50365	657	75.95	18	1.05	2.51
50421	727	84.05	20	1.25	2.82

Run	49		length	1393	mm
st. t.	6.46.661		heigth	39	mm
Time	x[mm]	x [%]	h[mm]	v[m/s]	Fr
46661	71	5.10	57		
46990	260	18.66	51	0.57	0.81
47155	378	27.14	46	0.72	1.06
47353	519	37.26	46	0.71	1.06
47551	699	50.18	43	0.91	1.40
47914	982	70.50	31	0.78	1.41
48013	1100	78.97	27	1.19	2.32
48144	1300	93.32	23	1.53	3.21

Run	53		length	735	mm
st. t.	4.11.398		heigth	50	mm
Time	x[mm]	x [%]	h[mm]	v[m/s]	Fr
12164	96		34		
12231	109	14.83	31	0.19	0.35
12298	136	18.50	27	0.40	0.78
12364	154	20.95	29	0.27	0.51
12431	165	22.45	26	0.16	0.33
12498	196	26.67	26	0.46	0.92
12564	228	31.02	25	0.48	0.98
12631	245	33.33	26	0.25	0.50
12698	270	36.73	25	0.37	0.75
12764	287	39.05	26	0.26	0.51
12831	321	43.67	24	0.51	1.05
12898	341	46.39	22	0.30	0.64

Run	48		length	536	mm
st. t.	6.07.225		heigth	19	mm
Time	X[mm]	x [%]	H[mm]	V[m/s]	Fr
7291	27	5.04	21		
7356	57	10.63	26	0.46	0.91
7455	94	17.54	25	0.37	0.75
7521	130	24.25	23	0.55	1.15
7587	170	31.72	21	0.61	1.34
7653	204	38.06	20	0.52	1.16
7719	242	45.15	17	0.58	1.41
7917	358	66.79	18	0.59	1.39
8049	420	78.36	15.5	0.47	1.20
8115	471	87.87	12	0.77	2.25
8181	515	96.08	10	0.67	2.13

Run	51		length	903	mm
st. t.	3.47.649		heigth	36	mm
Time	x[mm]	x [%]	h[mm]	v[m/s]	Fr
48176	229	25.36	43		
48275	254	28.13	43	0.25	0.39
48374	282	31.23	42	0.28	0.44
48506	311	34.44	42	0.22	0.34
48671	362	40.09	40	0.31	0.49
48835	409	45.29	29.5	0.29	0.53
49001	456	50.50	25	0.28	0.57
49066	485	53.71	21	0.45	0.98
49462	650	71.98	20	0.42	0.94
49528	700	77.52	18	0.76	1.80
49561	720	79.73	17	0.61	1.48
49594	755	83.61	13	1.06	2.97
49627	790	87.49	12	1.06	3.09
49660	830	91.92	11	1.21	3.69

Run	54		length	721	mm
st. t.	4.26.998		heigth	61	mm
Time	x[mm]	x [%]	h[mm]	v[m/s]	Fr
26998	149	20.67	27.5		
27031	155	21.50	27.5	0.18	0.35
27065	166	23.02	27.5	0.32	0.62
27131	191	26.49	27.5	0.38	0.73
27198	210	29.13	27.5	0.28	0.55
27265	232	32.18	26	0.33	0.65
27331	245	33.98	26	0.20	0.39
27398	273	37.86	32	0.42	0.75
27498	305	42.30	31	0.32	0.58
27631	359	49.79	27.5	0.41	0.78
27731	375	52.01	26	0.16	0.32
27798	396	54.92	23	0.31	0.66

12964	376	51.16	20	0.53	1.20
13031	415	56.46	16	0.58	1.47
13098	480	65.31	14	0.97	2.62

Run	56		length	834	mm
st. t.	10.18.825		heigth	70	mm
Time	x[mm]	x [%]	h[mm]	v[m/s]	Fr
18792	369	44.24	21		
18825	378	45.32	21	0.27	0.60
18859	395	47.36	21	0.50	1.10
18892	414	49.64	20	0.58	1.30
18925	435	52.16	18	0.64	1.51

Run 56 is continued on the right..

27831	408	56.59	19	0.36	0.84
27898	443	61.44	13	0.52	1.46
27965	472	65.46	12	0.43	1.26
28032	531	73.65	17	0.88	2.16
28098	601	83.36	16	1.06	2.68

Run 56 continued..

18959	453	54.32	16	0.53	1.34
18992	468	56.12	17	0.45	1.11
19025	490	58.75	16	0.67	1.68
19125	553	66.31	13	0.63	1.76
19192	615	73.74	12.5	0.74	2.10
19325	743	89.09	13	0.96	2.69

Next to these, a series of runs, done by Cartigny, are used, where the discharge could be measured using flow velocity sensors in a different set up. These are runs M4, M5, M6, M9 and M10. Dividing the discharge by the flume width gives the specific discharge, which is used to create a velocity profile along the bed by dividing it by the local flow depth. Since we are interested in the Froude number, the flow velocity and flow depth are used in formula 1, resulting in the Froude number distribution along a cyclic step (Table 3.3).

<Table 3.3 (below), Froude number distribution is calculated by using the specific discharge and the measured flowdepth along a step. Per run the name, the time of the logged image when measuring for this data started, the step length and height, the bedslope and the specific discharge is given. Depending on the desired resolution, measurement points are taken in steps between 50 and 150 mm. The distance 'x' is measured from the deepest point in a scour downstream. Also the relative position 'x' is given, with the step length as 100%. The flow depth 'h' is given for every measurement point. The local flow velocity 'v' is given in meters per second.>

Run	M4		Slope	2.2
St. time	3.01.770		High. P.	950
length	2200	mm	q	0.07
height	129	mm		
x [mm]	x [%]	h [mm]	v [m/s]	Fr.
0	0.00	148	0.47	0.39
100	4.55	144	0.49	0.41
200	9.09	138	0.51	0.44
300	13.64	130	0.54	0.48
400	18.18	115	0.61	0.57
450	20.45	107	0.65	0.64
500	22.73	97	0.72	0.74
550	25.00	89	0.79	0.84
600	27.27	88	0.80	0.86
650	29.55	92	0.76	0.80
700	31.82	88	0.80	0.86
750	34.09	79	0.89	1.01
800	36.36	75	0.93	1.09

Run	M5		Slope	3
St.time	1.19.430		High. P.	1360
length	2565	mm	q	0.07
height	215	mm		
x [mm]	x [%]	h [mm]	v [m/s]	Fr.
0	0.00	195	0.36	0.26
100	3.90	183	0.38	0.29
200	7.80	179	0.39	0.30
300	11.70	164	0.43	0.34
400	15.59	150	0.47	0.38
500	19.49	148	0.47	0.39
600	23.39	131	0.53	0.47
700	27.29	117	0.60	0.56
750	29.24	109	0.64	0.62
800	31.19	99	0.71	0.72
850	33.14	96	0.73	0.75
900	35.09	86	0.81	0.89
950	37.04	84	0.83	0.92

850	38.64	72	0.97	1.16
900	40.91	63	1.11	1.41
950	43.18	61	1.15	1.48
989	44.95	59	1.19	1.56
990	46.50	66	1.06	1.32
991	47.77	65	1.08	1.35
992	48.95	63	1.11	1.41
993	50.45	62	1.13	1.45
994	51.86	63	1.11	1.41
996	53.36	56	1.25	1.69
997	54.86	54	1.30	1.78
998	56.41	52	1.35	1.88
1267	57.59	50	1.40	2.00
1280	58.18	46	1.52	2.27
1310	59.55	44	1.59	2.42
1340	60.91	43	1.63	2.51
1370	62.27	42	1.67	2.60
1400	63.64	41	1.71	2.69
1430	65.00	40	1.75	2.79
1460	66.36	39	1.79	2.90
1500	68.18	38	1.84	3.02
1550	70.45	46	1.52	2.27
1600	72.73	51	1.37	1.94
1700	77.27	77	0.91	1.05
1800	81.82	117	0.60	0.56
1900	86.36	111	0.63	0.60
2000	90.91	150	0.47	0.38
2100	95.45	144	0.49	0.41
2200	100.00	158	0.44	0.36

Run	M6		Slope	4
St. time	2.30.000		Highest p	980
length	2100	mm	q	0.082
height	250	mm		
x [mm]	x [%]	h [mm]	v [m/s]	Fr.
0	0.00	228	0.36	0.24
100	4.76	220	0.37	0.25
200	9.52	216	0.38	0.26
300	14.29	201	0.41	0.29
400	19.05	182	0.45	0.34
500	23.81	155	0.53	0.43
600	28.57	126	0.65	0.59
700	33.33	110	0.75	0.72
800	38.10	114	0.72	0.68
900	42.86	101	0.81	0.82
950	45.24	85	0.96	1.06
1000	47.62	81	1.01	1.14
1100	52.38	76	1.08	1.25
1200	57.14	66	1.24	1.54
1300	61.90	66	1.24	1.54
1000	38.99	86	0.81	0.89
1050	40.94	78	0.90	1.03
1100	42.88	74	0.95	1.11
1150	44.83	66	1.06	1.32
1200	46.78	62	1.13	1.45
1250	48.73	58	1.21	1.60
1300	50.68	51	1.37	1.94
1400	54.58	49	1.43	2.06
1500	58.48	41	1.71	2.69
1600	62.38	35	2.00	3.41
1700	66.28	37	1.89	3.14
1800	70.18	39	1.79	2.90
1900	74.07	57	1.23	1.64
2000	77.97	76	0.92	1.07
2100	81.87	133	0.53	0.46
2200	85.77	160	0.44	0.35
2300	89.67	183	0.38	0.29
2400	93.57	201	0.35	0.25
2500	97.47	236	0.30	0.19
2565	100.00	261	0.27	0.17

Run	M9		Slope	0.5
length	3750	mm	High. P.	2.78
height	40	mm	q	0.0969
x [mm]	x [%]	h [mm]	v [m/s]	Fr.
0	0	139	0.70	0.60
150	4	132	0.73	0.65
300	8	145	0.67	0.56
450	12	152	0.64	0.52
600	16	158	0.61	0.49
750	20	171	0.57	0.44
900	24	176	0.55	0.42
1050	28	193	0.50	0.36
1200	32	200	0.48	0.35
1350	36	178	0.54	0.41
1500	40	158	0.61	0.49
1650	44	139	0.70	0.60
1800	48	139	0.70	0.60
1950	52	130	0.75	0.66
2100	56	115	0.84	0.79
2250	60	104	0.93	0.92
2400	64	89	1.09	1.17
2550	68	82	1.18	1.32
2700	72	78	1.24	1.42
2850	76	69	1.40	1.71
3000	80	60	1.62	2.11
3150	84	56	1.73	2.33
3300	88	47	2.06	3.04
3450	92	45	2.15	3.24
3600	96	39	2.48	4.02

1400	66.67	58	1.41	1.87
1500	71.43	62	1.32	1.70
1600	76.19	101	0.81	0.82
1700	80.95	160	0.51	0.41
1800	85.71	195	0.42	0.30
1900	90.48	218	0.38	0.26
2000	95.24	241	0.34	0.22
2100	100.00	264	0.31	0.19

Run	M10		Slope	3.5
length	2500	mm	Highest p	1280
heigth	235	mm	q	0.0762
x [mm]	x [%]	h [mm]	v [m/s]	Fr.
0	0	139	0.55	0.47
100	4	143	0.53	0.45
200	8	136	0.56	0.49
300	12	134	0.57	0.50
400	16	136	0.56	0.49
500	20	141	0.54	0.46
600	24	113	0.67	0.64
700	28	104	0.73	0.73

Run 10 is continued on the right..

3750	100	76	1.28	1.48

Run 10 continued..

800	32	100	0.76	0.77
900	36	106	0.72	0.70
1000	40	108	0.71	0.69
1100	44	110	0.69	0.67
1200	48	102	0.75	0.75
1300	52	93	0.82	0.86
1400	56	82	0.93	1.04
1500	60	76	1.00	1.16
1600	64	67	1.14	1.40
1700	68	56	1.36	1.84
1800	72	56	1.36	1.84
1900	76	47	1.62	2.39
2000	80	37	2.06	3.42
2100	84	116	0.66	0.62
2200	88	167	0.46	0.36
2300	92	180	0.42	0.32
2400	96	213	0.36	0.25
2500	100	214	0.36	0.25

Pictures are taken from the logged video images for a try to visually determine relations between the regional slope and the Froude number on the highest point (Appendix A). The bed and water surface are traced and horizontal and regional slope reference lines are drawn. The critical point (i.e. Fr = 1) is pointed out on the images. A conclusion is drawn that visually analyzing the images on relations is hard, so the data had to be subtracted from the images and plotted.

The Froude numbers on the highest points, with the horizon as reference, and corresponding run name, regional slope and relative position are taken from tables 3.2 and 3.3 and given in table 3.4. The relation of the regional slope with the Froude number on the highest point of a step becomes visible when plotting them against each other (Figure 3.1) resulting in a relation (formula 2).

Run	slope	x%	Froude no.
48	0.5	60	1.4
49	0.8	55	1.4
51	1.4	71	1.5
56	1.7	50	1.3
53	2	50	1.15
M4	2.2	50	1.44
54	2.5	49	0.78
M5	3	55	2
44	3.4	49	1
M10	3.5	49	0.75
M6	4	48	1.15

<Table 3.4 (previous page), Slope versus the Froude number on the highest point. The run number, the slope in degrees, the distance of the highest point from the downstream trough in percentage of the step length and the Froude number are given.>

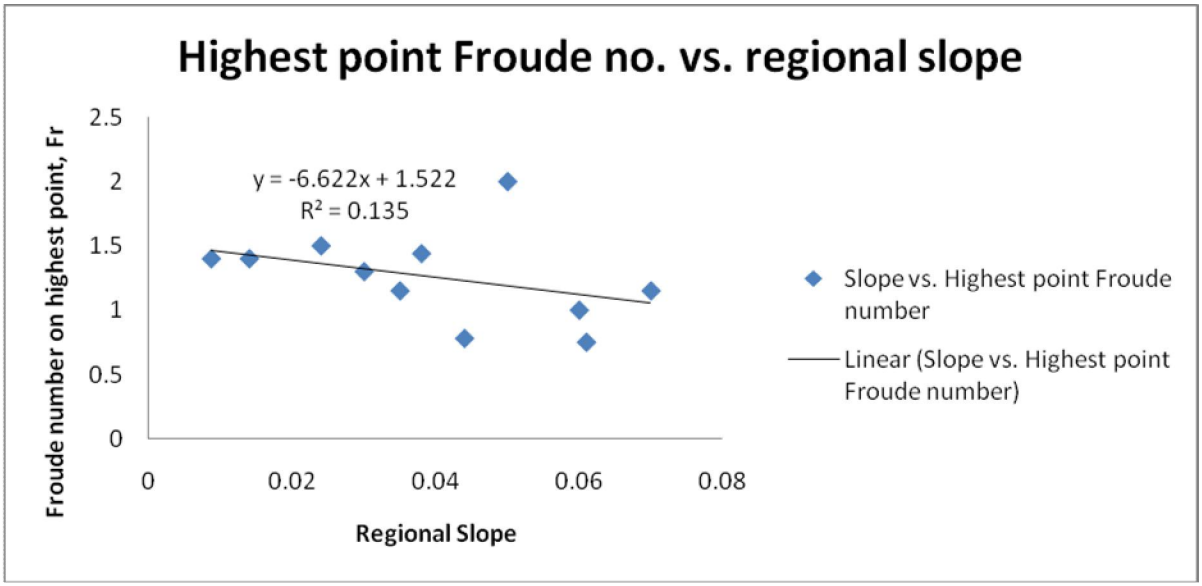

<Figure 3.1, Froude number on the highest point with the horizon as reference vs. regional slope.>

$$Fr_h = -6.622 i_r + 1.522 \qquad (2)$$

From formula two follows that an increase in slope decreases the Froude number on the highest point and when the regional slope is equal to 0.064, the critical point (i.e. Fr = 1) is the highest point.

Although, the function gives a good relation, the error on individual measurements might be large (R^2=0.135). One of the reasons is a listric faulting event that occurs intermittently trough time. An event is observed that makes the location of the highest point shift. Small listric faults and shear movements with a minor displacement developed during runs displacing the top part of the cyclic step in the downstream direction (figure 3.2). The step has a more rectangular shape when listric faulting did not occur for a while. Once one listric fault alters the slope, immediately a second one and a third one develop upstream. After this event, the shape of the step is more rounded and builds up again to a more rectangular shape.

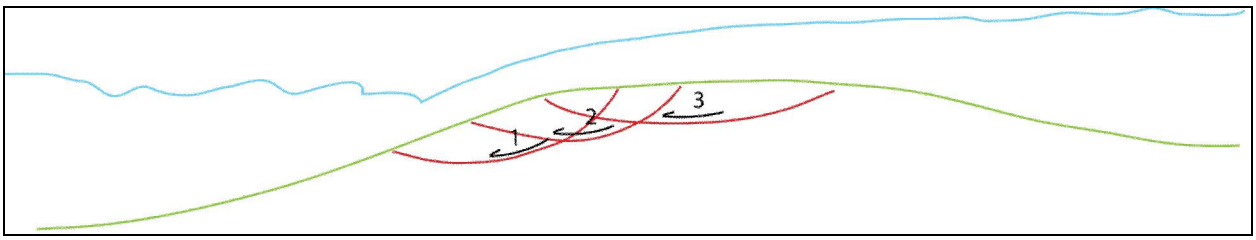

<Figure 3.2 (previous page), Schematic drawing of listric faults on a step. First the steep lee slope collapses (1). This is followed by 2 or 3 new listric faults (2, 3) and shear movements. The event takes place within one second. The flow is from right to left.>

Uncertainties in the collected data

No wall correction factor is used. Vanoni & Brooks (1957) used a wall correction factor to recalculate the shear stresses applied to a flow in a flume. Since I use the streampower calculated by the momentum balance, using observed values for flow velocity and flow depth, no friction or shear stresses has to be recalculated. It is unknown how the flume walls influence the results of the experiments.

Measurements of the flow depth at the highest point of a cyclic step have a maximum standard error of 1.69 mm. The error is determined from five different runs, by measuring the flow depth four times (Table 3.5). It results from the resolution of the cameras and of manually setting the screen measuring tool at the right position on the flow and bed edges. Because the resolution does not change for different flow depths, the standard error is an absolute value. Hence, the flow depth has a maximum standard error of 1.69 mm, which means greater flow depths have a smaller standard error in percentages.

	A	B	C	D	E
	11	23	36.7	13.1	6.6
	16.3	21.3	41	13.1	6.6
	13.14	21.3	32.8	16.4	6.5
	15	23	37.8	19	8.1
Average	13.86	22.15	37.075	15.4	6.95
Std.dev.	2.305877	0.981495	3.383662	2.86007	0.768115
Std.err.	1.152938	0.490748	**1.691831**	1.430035	0.384057
Std.Err.%	8.318458	2.215565	**4.563266**	9.285941	5.526004

<Table 3.5, five different flow depths (A-E) from different runs are measured 4 times. Values are in mm.>

The average velocity from run 42 to 57 is calculated using the displacement of a tracer per unit of time. As tracer a pigment with a high contrast, as described in the methodology, is added at the upstream end of the flume into the flow. When the tracer enters the recorded video image, a reference point is set and the time is notated in milliseconds. When the tracer in the flow is almost leaving the recorded video image, a second reference point is made, at the same place on a bedform as the first reference point. I.e. they are both set at the highest points of antidunes, or, in the case of cyclic steps, in the troughs. The difference in distance is divided by the difference in time. Since the time is logged in milliseconds within the movie by the software and the distance is measured using a screen measuring tool, the error will be relatively small compared to the error of visually determining the front of the cloud. As the tracer cloud enters the logged image, its cloud is highly concentrated and has therefore a high contrast. At the end of the logged image, the tracer cloud is a bit vague due to mixing and mistakes could be made. After looking at different tracer clouds, it is reasonable to say that the error on the average flow velocity, made by visual determining the front of the tracer cloud, could go up to 10% along the glass wall.

Measurements for the average flow depth is done by measuring the flow depth ten times equally distributed along a step, see figure 2.6. From these ten measurements the average is taken as average flow depth. To calculate the standard error, six different measurements (A to E) of the same run are done. This gives the standard error on the reproduction of the average flow depth. These are analyzed in table 3.6 and give a standard error of ~0.52 mm. Note that this is about the *average* flow depth measurements.

	A	B	C	D	E
1	19.5	21.3	24.4	19.0	21.0
2	20.1	20.1	20.2	21.9	20.6
3	20.6	19.1	19.0	20.1	19.7
4	26.2	20.6	26.2	22.7	23.9
5	29.9	26.2	24.3	26.2	26.6
6	41.2	39.3	37.4	39.3	39.3
7	50.5	44.9	44.9	44.9	46.3
8	59.8	56.1	54.2	54.2	56.1
9	59.8	57.9	57.9	54.2	57.5
10	52.3	46.7	48.6	48.6	49.1
AVG H	38.0	35.2	35.7	35.1	36.0

std.dev.	1.170534
std.err	0.523479

<Table 3.6, six different measurements (A-E) of the average flow depth (AVG H) on the same step, giving the standard error. The flow depth is measured 10 times, equally distributed, along a step. Values are in mm.>

The step height and length are determined with the screen measuring tool (MB-Ruler). Taking five measurements on two different steps from different runs gave a standard error of 0.6% for the length and 1.4% for the height. Table 3.7 shows the calculations on the measurements to come up with the error.

To reproduce the slope measurement and come up with the standard error on it, five measurements have been made of the slope in front of the cameras view. Depending on the measurement point, the slope of the flume varies with an error of 0.1°. With the slope of the flume known, with its error of 0.1°, the logged image can be analyzed to calculate the slope of the bedforms. This is done five times, see table 3.8. The total standard error on the slope is the Flume slope measurement error plus the bed slope measurement error, which comes to a total of 0.14°.

	Run 44, 7:34.674		Run 57, 5:42.062	
	L	h	L	h
	1138	56.8	446	24.5
	1151	58.1	451	23.4
	1162	57.9	459	24.6
	1172	57.3	444	22.9
	1169	57.1	450	24.4
Average	1158.4	57.44	450	23.96
st.dev.	13.97498	0.545894	5.787918	0.763544
std.err	6.2498	0.244131	2.588436	0.341467
std.err.%	0.53952	0.425019	**0.575208**	**1.425156**

<Table 3.7, The percentage of standard error is calculated from five measurements of the length and the height of two different steps. Values are in mm.>

Run 57, 6:01.362. Flume slope: 3.0°					
d1	h1	d2	h2	Distance	slope
127.5	99.4	112.5	67.3	2360	3.77
129.4	97.5	109.4	69.8	2361.2	3.67
136.9	97.5	110.6	72.3	2352.5	3.61
127.5	101.2	106.2	69.2	2366.3	3.77
125.6	105	109.4	71.1	2365	3.82

average	3.728
st.dev.	0.085557
std.err	0.038262

<Table 3.8, The standard error of the slope is calculated from five measurements between two reference points shown in figure 3.4>

The error on the streampower is a sum of several uncertainties and assumptions. Assuming the water density is 1, the sediment density is 2.65 g/cm^3 and the gravitational acceleration is 9.81 m/s^2. The flow velocity is calculated, using the Froude number on the highest point of a step. From figure 3.1 can be observed that around 80% of the measured values are within an error of 25%, which is hereby taken as error. Measuring the flow depth with a maximum error of 9.3% and the slope with a maximum error of 1%, combined with the calculated flow velocity with an error of 25% gives a total error for the streampower of 35.3 %. Around 80% of the errors will be within this range, of which the largest part will be more accurate.

Interpretation

The cyclic step geometry

To meet the first objective "Relate flow characteristics to the cyclic step geometry, so that palaeoflow conditions can be determined from deposits", the bedform parameters need to be analyzed on sensitivity for flow parameters.

The cyclic step geometry parameters (figure 2.1) are:

- Step height h_s [m] (Appendix C);
- Step length l_s [m] (Appendix D) ;
- Location of the highest point x_s [%] (Appendix F);
- Regional slope l_r [degrees] (Appendix G);

The cyclic step bedform parameters are analyzed on sensitivity for the following flow parameters:

- Flow specific discharge q [m^2/s] (product of flow velocity U [m/s] and flow depth h [m]);
- Streampower P [-];
- Flow sediment volume concentration c [%];
- Froude number Fr [-];
- Mobility parameter θ' [-];
- Relative flow depth h/D_{50} [-];

In all plots 0.320, 0.263, 0.185 and 0.118 mm median grain sizes are given. The 0.185 mm median sediment grain size experiments are done by Cartigny, who used higher discharge values in another flume configuration.

The flow parameters analyzed for the cyclic step bedform are included in Appendices C to G. The flow specific discharge and sediment concentration show a relation for the cyclic step length, but not for the cyclic step height.

The Froude number, the mobility parameter and the relative flow depth are using average values for the flow depth, of which its measurement method is described in the methodology. The flow depth along a step varies from a deeper section in the subcritical pool, to a shallow section at the supercritical chute. This makes the average flow depth values useless as distinction factor. This is due to the fact that more supercritical flows have more extreme hydraulic jumps. A higher Froude number at the end of a cyclic step corresponds to a lower Froude number at the beginning of a step, giving same values for less supercritical flows. Taking the average along a cyclic step for velocity or flow depth is therefore not used resulting that the Froude number, mobility parameter and relative flow depth cannot be used.

The Streampower gives a relation for the cyclic step height (figure 4.1a; formula 7) and cyclic step length (figure 4.1b; formula 8). No relation could be found for the location of the highest point, which is probably due to the listric faulting events (figure 3.2). The regional slope could not be related to flow

characteristics, which can now be explained by the fact that all parameters that describe the streampower influence the cyclic step geometry, of which the regional slope is only one.

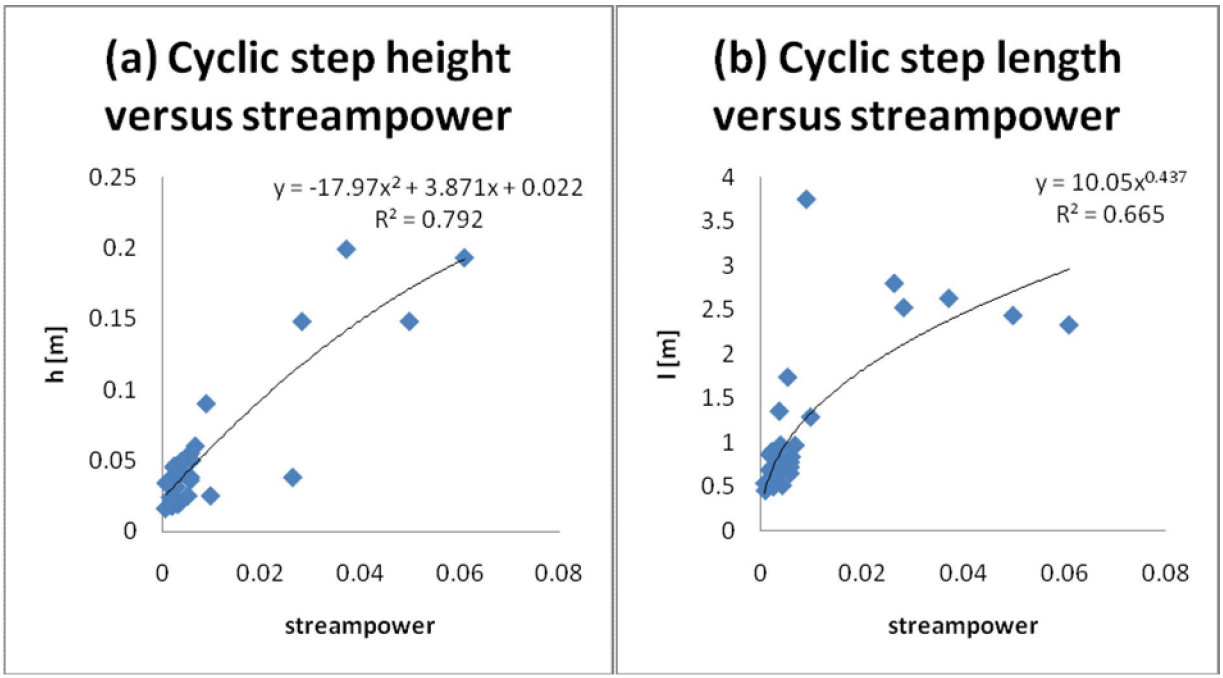

<Figure 4.1, (a) The cyclic step height versus streampower resulting in formula 7. (B) The cyclic step length versus streampower resulting in formula 8.>

$$h_s = -17.97\mathrm{P}^2 + 3.871\mathrm{P} + 0.022 \quad (7)$$

$$l_s = 10.05\mathrm{P}^{0.437} \quad (8)$$

The aspect-ratio of the cyclic step versus the streampower could be a useful parameter in the field. A plot is made (Appendix E) to investigate this. It appears that the streampower has no clear influence on the aspect-ratio. If all streampower values would end up within the same range of aspect-ratio values, the cyclic steps are scaled for changing streampower values. Instead of this, all streampower values are within the same range and the aspect-ratio varies. This suggests that other parameters influence the cyclic steps aspect-ratio. This also is not true, because I just proved that Streampower predicts the cyclic step height and length. This leaves me to conclude that the error on my data is too large to come up with a relation for the aspect-ratio.

The median sediment grain size could not be used, because exactly the same flow characteristics are needed to observe a relation in the cyclic step geometry for changing median sediment grain sizes. As explained in the results and what will also be discussed in “suggestions for further research” is that the flume configuration was not suitable for these tests, because the regional slope and the flow discharge

had to be set. A configuration where only the flow discharge or mixture discharge is set can help finding the relation between cyclic step geometry on changing median sediment grain size.

In Appendix A, Runs 48, 49, 51 and 51-2 show normal hydraulic jumps and runs 44, 53, 54, 56, M4, M5, M6 and M10 show submerged hydraulic jumps. Their regional slope and type of hydraulic jump is summarized in table 4.1.

(A.1) Lee side slope per run		
run	Regional Slope	Jump
48	0.5	normal
49	0.8	normal
51 / 51-2	1.4	normal
44	3.4	submerged
53	2	submerged
54	2.5	submerged
56	1.7	submerged
M4	2.2	submerged
M5	3	submerged
M6	4	submerged
M10	3.5	submerged

<Table 4.1, A summary of the cyclic steps shown in Appendix A, with their run number, regional slope and state of the hydraulic jump.>

Cyclic steps with a submerged hydraulic jump have a well developed pool, in contrast to cyclic steps with a normal hydraulic jump. A parameter that separates the normal hydraulic jump from the submerged hydraulic jump is the regional bed slope. All normal hydraulic jumps are formed on a maximum regional slope of 1.4 degrees, while the submerged hydraulic jump is formed with a regional slope with a minimum of 1.7 degrees.

Objective one “relate flow characteristics to the cyclic step geometry, so that palaeoflow conditions can be determined from deposits” is met. The palaeo flow conditions, in terms of the streampower, can now be calculated when the cyclic step length or height can be determined from the geological record. If the regional slope can be reconstructed from the geological record, the state of the hydraulic jump from the palaeo flow of the cyclic steps can be termed normal or submerged.

The definition for cyclic steps

To meet the second goal “to sharpen the definition for cyclic steps”, the results from the first aim are used. In this research the term cyclic step is used as described by Fukuoka et al. (1982). The term chute-and-pool from Fukuoka et al. (1982 in Taki and Parker, 1995) corresponds to the description given by Cartigny et al. The two definitions of cyclic steps:

Taki & Parker (1995):

> "The first to describe them was Fukuoka et al. (1982) who described the Chute and Pool morphology as a limiting case of cyclic steps for which the steepest bed slope realized just upstream of the hydraulic jump is still rather mild. The term 'cyclic steps' is used for the entire class of spatially periodic bedforms, where each wavelength is delineated by an upstream and downstream hydraulic jump."

Cartigny et al. (2009):

> "If a bore becomes stationary relative to a knick point, the bore will be called a hydraulic jump. Such a hydraulic jump can take three positions relative to a knick point: 1) upstream of the knick point, forming a cyclic step 2) at the knickpoint, a chute-and-pool is formed 3) after the knick point, forming a transverse rib."

Chute-and-pool structures have rather mild slopes just upstream of the hydraulic jumps, which are related to normal hydraulic jumps. A cyclic step with a submerged hydraulic jump goes together with a relatively steep slope just upstream of the hydraulic jump (see figure 1.1). To determine if the slope just upstream of a hydraulic jump is rather mild is relatively hard, see e.g. Appendix A. Also, the term 'rather mild' is a vague description.

The processes that play at the formation of chute and pools and cyclic steps are the same, only the state of the hydraulic jump differs. In order to remove confusion in terminology, I suggest using the term cyclic steps for the entire class of spatially periodic bedforms, where each wavelength is delineated by an upstream and downstream hydraulic jump, with the additional information of the state of the hydraulic jump, which can be normal or submerged.

Bedform stability diagram for the upper flow regime.

The data produced is used to create a bedform stability diagram. The bedform stability diagram has to extend proven bedform stability diagrams in the upper flow regime. The bedform stability diagrams that have proven successful show upper plane bed and antidunes, but exclude cyclic steps. Upper plane bed and antidune data from others (Appendix B) will be used in combination with the data produced in this study to try to find a relation between the bedforms of the upper flow regime.

Antidunes are not a stable bedform (Simons et al., 1965; Cartigny et al., 2009; pers. comm. Dr. Van den Berg) and cycle between upper plane bed and breaking antidunes. They can travel up- or downstream and can be called standing waves when they keep their position. They are related to the Froude number and form when it is around one. This means that the zone in which the antidunes form most likely overlaps other bedform zones when plotting on flow characteristics other than the Froude number. Runs have been conducted that did not show stable bedforms, but an alteration of cyclic steps and antidunes. I relate this situation to the zone, where streampower values are within the cyclic step zone and the Froude number is around one.

In this study the streampower predicts the cyclic step geometry and will therefore be used in a bedform stability diagram for the upper flow regime. A diagram where streampower and median sediment grain size are used is from Simons and Richardson (1966). This diagram is analyzed to do a prediction for the formation of cyclic steps within the tested range. For the range of median sediment sizes from 0.100 to 0.350 mm, the ripple to dune transition is around the streampower value of 1 (figure 4.2 B, where 0.100 and 0.350 mm median sediment sizes are indicated with blue lines). Upper plane bed develops with increasing streampower (from 5 to 8) for increasing median sediment grain size (from 0.100 to 0.350 mm). Antidunes start to develop for every median sediment grain size at the same flow values. Bed characteristics, like the median sediment grain size, do not influence antidunes and are only predicted by the Froude number. I therefore expect that the formation of cyclic steps shows a similar relation between streampower and median sediment grain size as the formation of upper plane bed. Data from other studies (Appendix B) have been added and plotted in a diagram (figure 4.3).

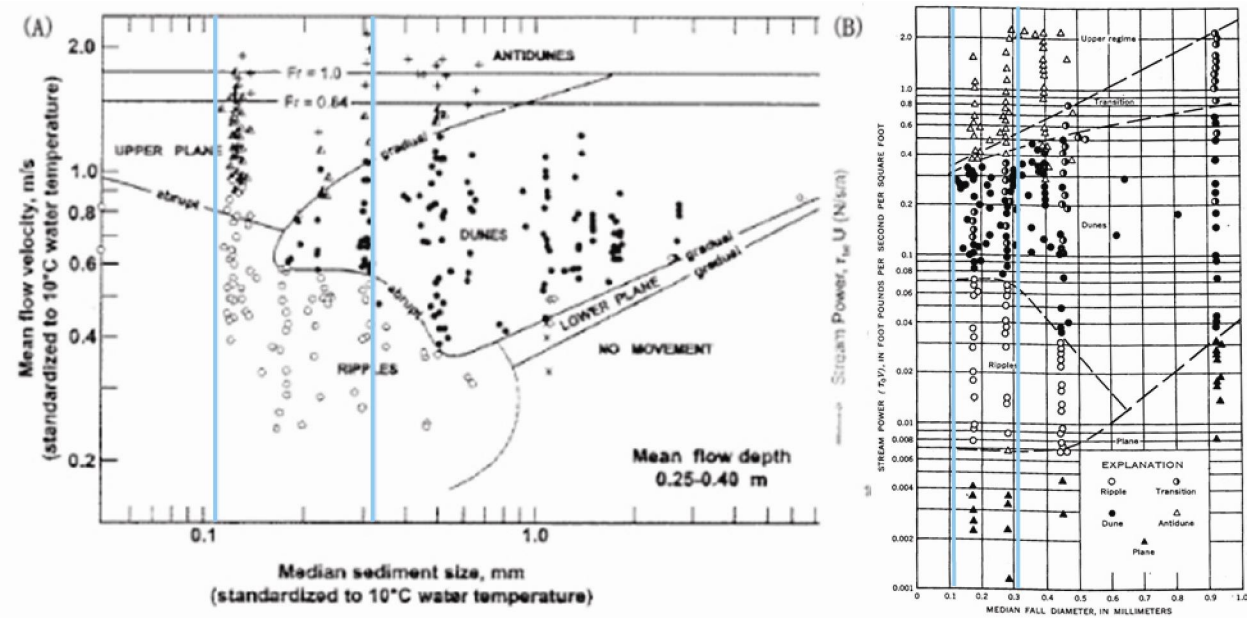

<Figure 4.2, (A) mean flow velocity versus median sediment size by Boguchwal & Southard adapted from Ashley (1990). (B) Streampower versus median fall diameter by Simons and Richardson (1966).Median sediment grain sizes of 0.118 and 0.320 mm have been highlighted with blue lines.>

Within the created diagram on streampower versus median sediment grain size (figure 4.3), the different bedforms overlap each other. The expected relation for the formation of cyclic steps cannot be proven, nor disproven, because of the absence of data for bedforms between median sediment grainsizes from 150 to 300 µm for streampower values between 0.002 and 0.006. Without this data it is unknown whether the formation of cyclic steps is dependent or independent on the median sediment grain size.

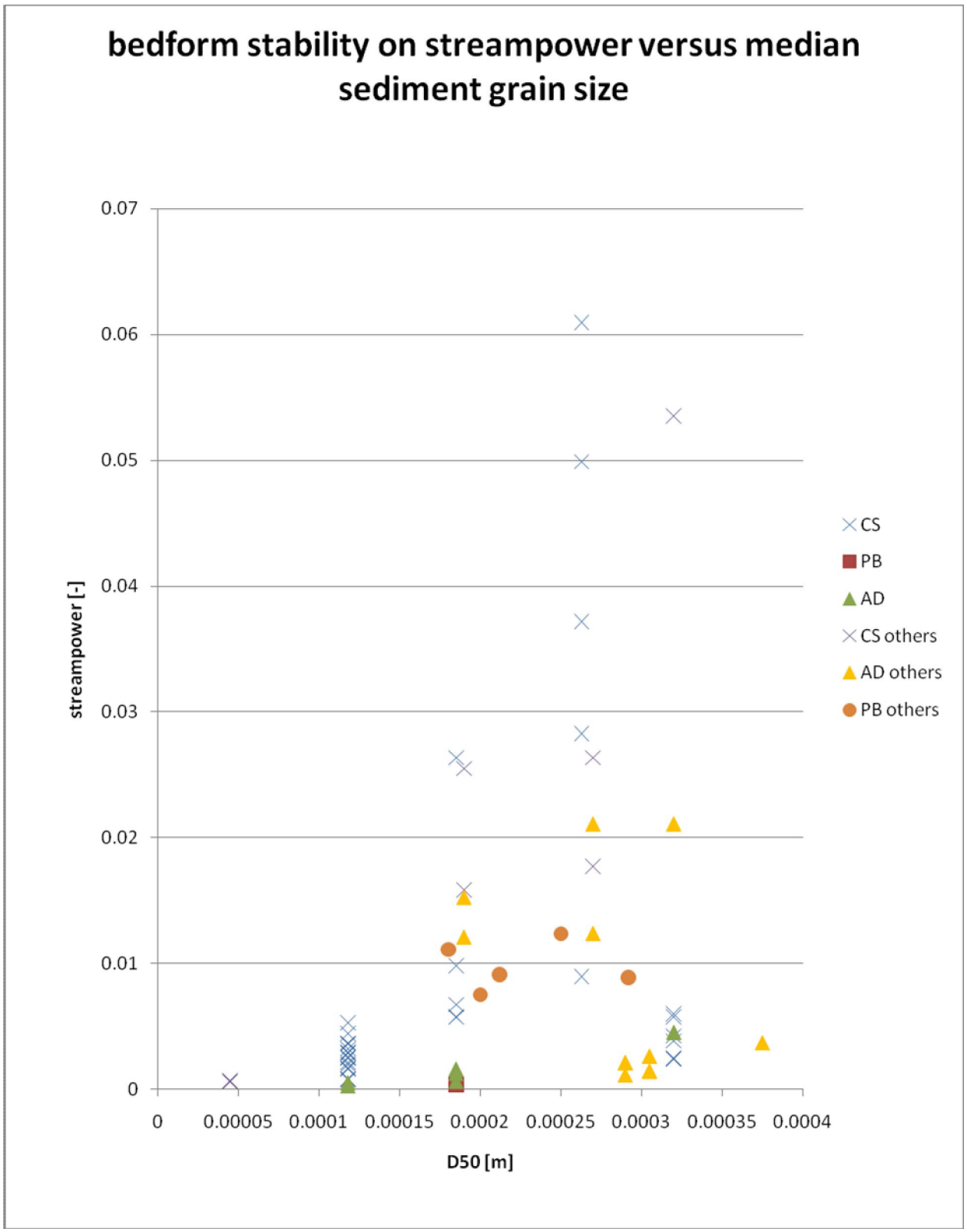

<Figure 4.3, Bedform stability diagram on streampower versus median sediment grain size. The data used is produced in this study (Table 3.1), together with data from others (Appendix B)>

Another parameter needs to be found that can make distinctions between the formation of the different bedforms. Since streampower appeared to be an important factor for the formation of cyclic steps, literature provides that streampower is the dominant factor in predicting sediment concentration (Yang et al., 1974). Plotting the bedforms in a diagram using the concentration separates the formation of the different bedforms from each other (figure 4.4). When considering antidunes as an unstable bedform, flat bed and cyclic steps are perfectly separated when using concentration versus median sediment grain size. However, concentration is a result from flow and bed characteristics and not a useful parameter in the geological record.

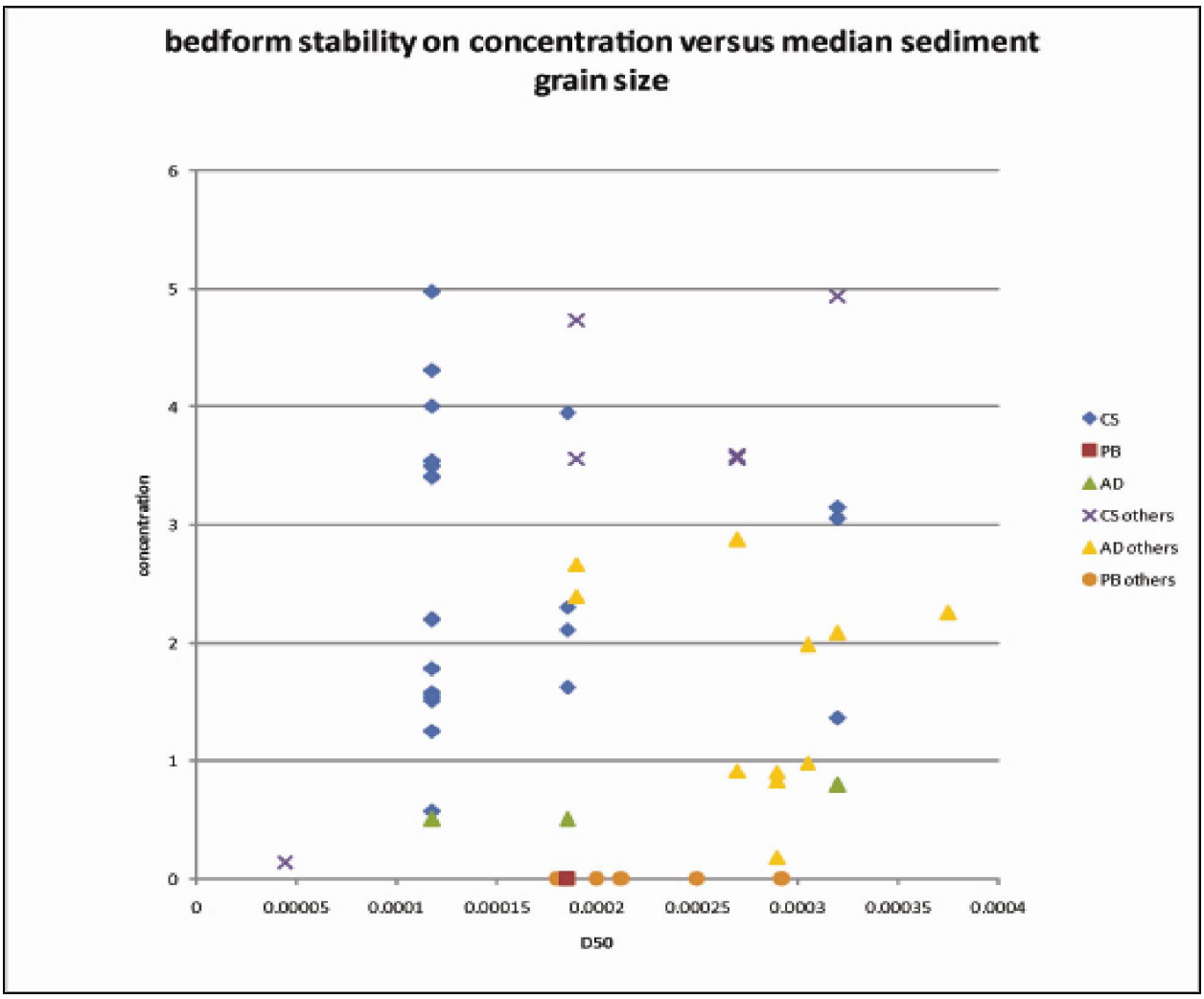

<Figure 4.4, Bedform stability diagram on sediment concentration versus median sediment grain size. The data used is produced in this study (table 3.1), together with data from others (Appendix B).>

Also attempts have been made to use other parameters, such as the mobility parameter, the Froude number and specific discharge (Appendix H), but appear not useful for a upper flow regime bedform stability diagram. The mobility parameter and Froude number use the flow depth, which varies for cyclic steps, and which also appeared not to be useful in the sensitivity analysis for the cyclic step geometry.

The specific discharge puts cyclic steps in the middle of the upper plane bed zone and can therefore not be used in a stability diagram for the upper flow regime.

The streampower plotted against slope (Figure 4.5) shows a better distinction for the different bedforms. In this diagram an interpreted blue line is drawn for the transition from plane bed to cyclic steps and between the transition of cyclic steps with a normal to a submerged hydraulic jump. Due to the lack of data with a slope between 1.4 and 1.7 degrees, the relation of the transition from cyclic steps with a normal and a submerged hydraulic jump is unknown. Therefore, the transition is drawn in the diagram with a question mark. The transition could be at the same slope for every streampower, or, like the transition from upper plane bed to cyclic steps, have a decreasing slope value for an increasing streampower. Antidunes are a bedform that forms when the Froude number is around one. This zone is overlapping both the cyclic steps and upper plane bed zones and is bounded by yellow dotted lines in the diagram.

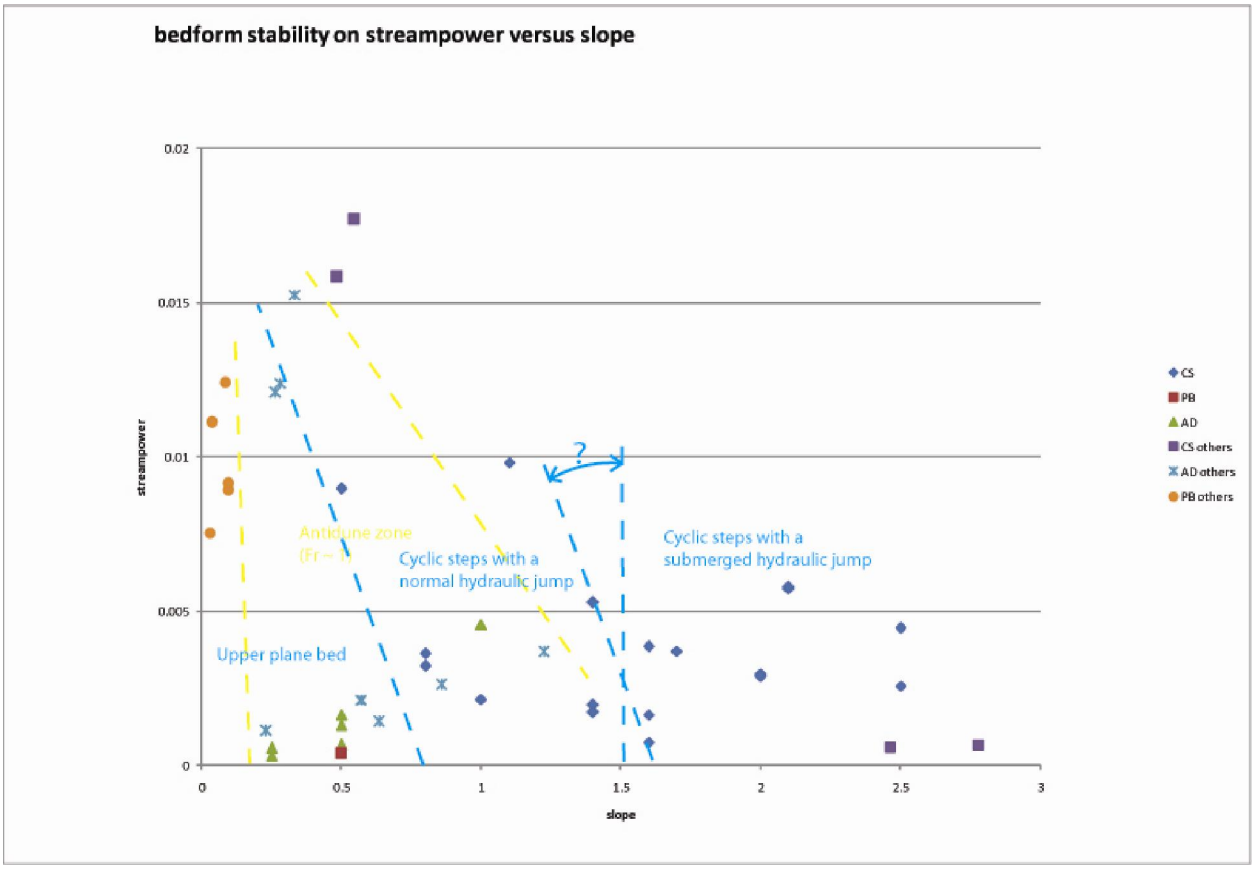

<Figure 4.5, bedform diagram with streampower versus slope. An interpretation has been made, with the dashed blue line separating plane bed from cyclic steps and dividing the cyclic steps with a normal from a submerged hydraulic jump. An overlapping antidune zone is indicated, bounded by the yellow dashed lines.>

This study did not focus on the lower flow regime bedforms that are characterized by bedload transport. If they have to be plotted within the stability diagram on streampower versus slope, they would be located at lower streampower values than upper plane bed (<0.75) with a maximum slope around 0.25.

Discussion

The results from this study, the expected relations that were not found and questions that remain unanswered will be discussed.

A summation of the results:

1. The Froude number on the highest point of a step, is described by formula 2;
2. The streampower gives a relation for the cyclic step height (figure 4.1a; formula 7) and cyclic step length (figure 4.1b; formula 8);
3. A new definition for cyclic steps is suggested, where this term is used for the entire class of spatially periodic bedforms, where each wavelength is delineated by an upstream and downstream hydraulic jump, with the additional information of the state of the hydraulic jump, which can be normal or submerged;
4. All normal hydraulic jumps are formed on a maximum regional slope of 1.4 degrees, while the submerged hydraulic jump is associated with a minimal regional slope of 1.7 degrees;
5. Antidunes start to develop for every median sediment grain size at same flow values, where the Froude number is around one. Bed characteristics, like the median sediment grain size, do not influence antidunes;
6. When considering antidunes as an unstable bedform, flat bed and cyclic steps are perfectly separated when using concentration versus median sediment grain size (figure 4.4). This creates a good upper flow regime bedform stability diagram.

Some expected results were not found and other questions arose during this study. These are:

7. The flow specific discharge and sediment concentration show a relation for the cyclic step length (Appendix D, plot A & B), but not for the cyclic step height (Appendix C, plot A & B). Is the relation expected and, if true, why was it not found?
8. For the aspect-ratio, as well as for the concentration, relations were expected with the streampower, but were not found. Why were they expected and why were they not found?
9. The streampower plotted against slope (Figure 4.5) shows a better distinction for the different bedforms. This is used for the final upper flow regime bedform stability diagram in this study. How does it relate to other bedform stability diagrams? Why is the streampower from Simons and Richardson (1966) a factor ~10^3 larger?

In the next section the summed subjects will be discussed.

1) The formula for the Froude number on the highest point of a cyclic step (formula 2) is used to determine the flow velocity. This parameter is very important for all data and has a relatively large uncertainty (R^2 = 0.135), which is caused by listric faulting on the cyclic steps, as discussed in the results section. Fildani et al. (2006) made calculations using a numerical model from Parker that also prove that the Froude number on the highest point of a cyclic step is reduced when the regional slope becomes

larger (pers. comm. Cartigny). This is the same relation I found, but still, this does not improve its accuracy.

2) The streampower gives a relation for the cyclic step height (formula 7) and length (formula 8). The relations have uncertainties, respectively an R^2 of 0.792 and 0.665. Streampower is expected to be the best parameter to describe the cyclic step geometry, because it includes all energy bearing parameters and is successfully used in the description of bedforms and sedimentary processes by Simons and Richardson (1966) and Yang et al. (1974). An increasing discharge increases the bedform length and height in the lower flow regime (Julien et al., 1995) and influences the streampower values, complementing the here found relation.

3) Two definitions for cyclic steps (Fukuoka et al. (1982) and Cartigny et al. (2009)) are discussed in the interpretation section. Based on the data of this study a new definition is suggested. The suggestive term "rather mild", as used by Fukuoka et al. (1982) to describe chute and pools, a subclass of cyclic steps, is quantified with a slope angle in this study. The new definition is improved and made more useful in practical situations.

4) All normal hydraulic jumps are formed on a maximum regional slope of 1.4 degrees, while the submerged hydraulic jump is associated with a minimal regional slope of 1.7 degrees. This corresponds to the studies of Guy et al. (1966), Fukuoka et al. (1982) and Cartigny et al. (2009), who pointed out that an increase of slope changes the state of the hydraulic jump.

5) Antidunes develop where the Froude number is around one (Boguchwal & Southard, 1990; Garcia, 2008). A conclusion is drawn in this study supported by the results, that median sediment grainsize does not influence the formation of antidunes. The Froude number is also sensitive for the density of the fluid, as described by the densiometric Froude number. However, the small density differences caused by the sediment concentration in the flow are hard to measure and would be too small to make a difference and could therefore be neglected in subaerial flows.

6) When considering antidunes as an unstable bedform, flat bed and cyclic steps are perfectly separated when using concentration versus median sediment grain size (figure 4.4). Antidunes are not a stable bedform (Simons et al., 1965; Cartigny et al., 2009; pers. comm. Dr. Van den Berg) and cycle between upper plane bed and breaking antidunes. Some of my Flume experiments show antidunes superimposed on cyclic steps, also observed by Alexander et al. (2001) and Cartigny et al. (2009). As discussed in point 5, subaerial antidunes form when the Froude number is around one. This means that the stability fields in which the antidunes occur overlaps with other bedform fields when plotting on flow characteristics other than the Froude number.

7) The flow specific discharge and concentration both show a relation for the cyclic step length and not for the height (Appendix C & D, plot A & B). The bedform length and height are both scaled by the discharge for the lower flow regime (Julien et al., 1995). Same relations were therefore expected for the upper flow regime. Water depth is shown to play a role in limiting dune growth in shallow water (Flemming, 2000). Subaerial cyclic steps are associated with very shallow water, which is probably the

reason why no relation for the cyclic step height can be found for the flow specific discharge and the flow sediment concentration.

8) Relations are found where the streampower predicts the cyclic step length and height. No relation is found for the aspect-ratio (Appendix E). The streampower is more or less scaling the bedform, as the discharge does for the lower flow regime (Julien et al., 1995). The relations from the cyclic step height (figure 4.1 A) and length (figure 4.1 B) are almost identical, which proofs that the whole step is scaled with the streampower and that no relation exists for the aspect-ratio.

Is my concentration value correctly measured? Winterwerp (1986) did flume experiments on the critical slope of cyclic steps. This is the minimal slope needed to produce cyclic steps with certain flow values, like concentration and discharge. His tested concentrations that produced cyclic steps vary from 3 % up to 30%. These values correspond to my values, which are between 0.6 and 12 %. Different input settings for concentration and discharge created the difference between the ranges of concentrations.

According to Yang et al. (1974) the streampower predicts the sediment concentration. In my results, the streampower in combination with the slope (figure 4.5) predicts the bedform, as well as the concentration in combination with the median sediment grain size (figure 4.4) predicts the bedform. When I plot streampower against concentration, no relation can be found in my data, while data from others shows the relation (figure 5.1).

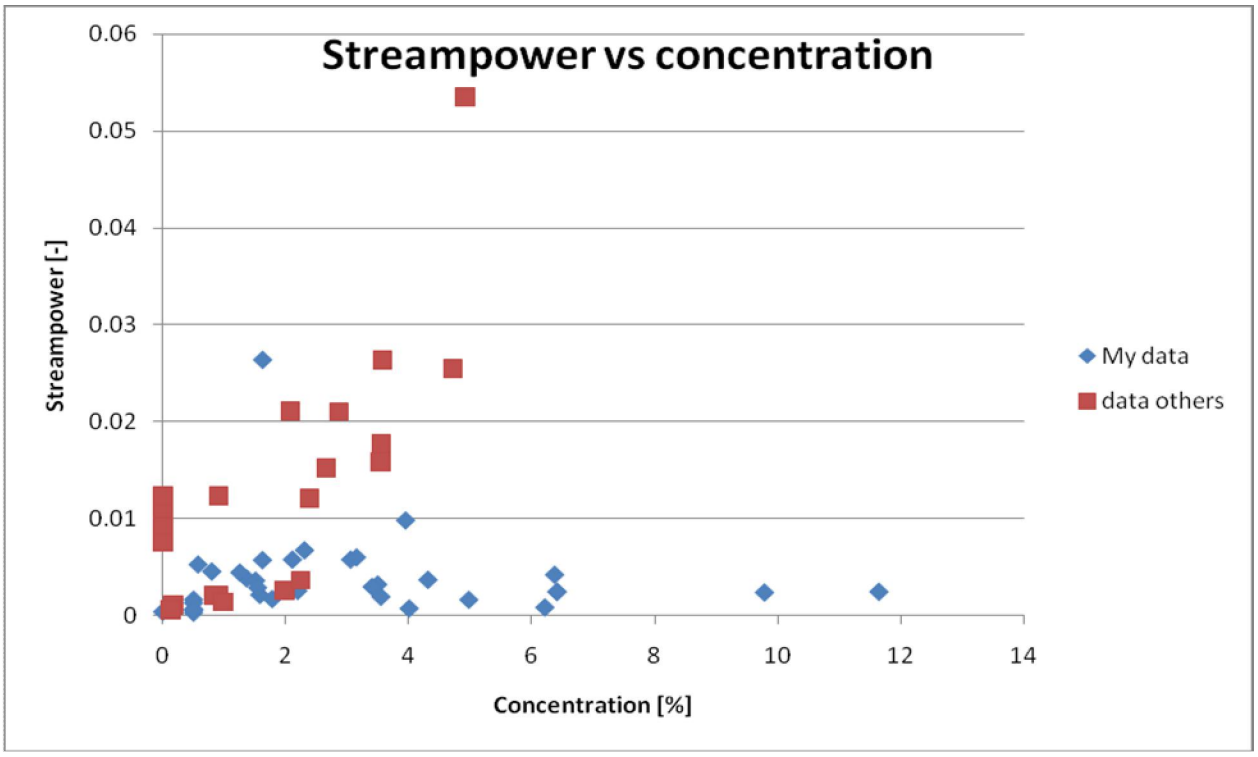

<Figure 5.1, Streampower versus concetration for my data and for the data of others shown in Appendix B.>

The reason why data from others does work, might be because most of it is natural river data, where an increasing streampower is caused by an increased specific discharge. My experiments are done using a low specific discharge, which is more or less the same for every run, while equilibrium slope of CS and sediment concentration vary. Since the slope and concentration have a minimal influence on the streampower, the relation could not be found with my data. The slope plotted against concentration shows that the slope has a strong influence on the flow sediment concentration in my experiments (figure 5.2).

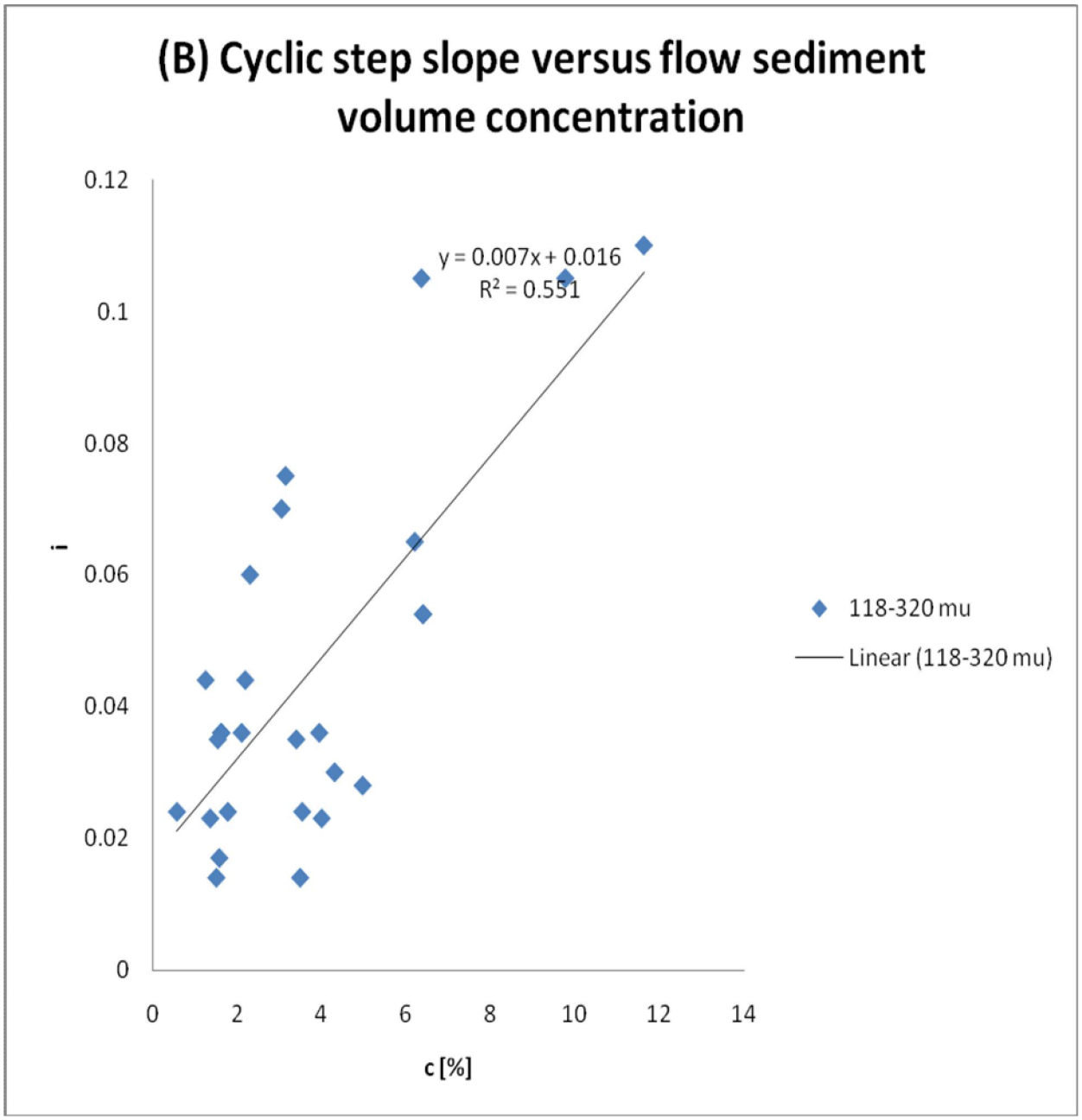

<Figure 5.2, Slope versus concentration with my data, showing that the slope has a strong influence on the flow sediment concentration.>

9) A good upper flow regime bedform stability diagram is made, using the streampower and the regional slope (figure 4.5). A comparison of the upper flow bedform stability diagram with other diagrams would be perfect to discuss it. Cyclic step data is available from natural rivers and flume experiments. However, no one created a bedform stability diagram that includes cyclic steps. A comparison can therefore not be made. The connection between a bedform stability diagram for the lower flow regime, such as the one of Simons and Richardson (1966; Figure 4.2 B), with the upper flow regime bedform stability diagram from this study can be compared. The units from Simons and Richardson (1966) are English and have to be converted. The conversion factor in the Streampower is 0.0103. The values from median sediment grain sizes from 0.112 to 0.320 mm are taken from the graph, converted and drawn in the bedform stability diagram of this study, where the slope is zero (figure 5.3).

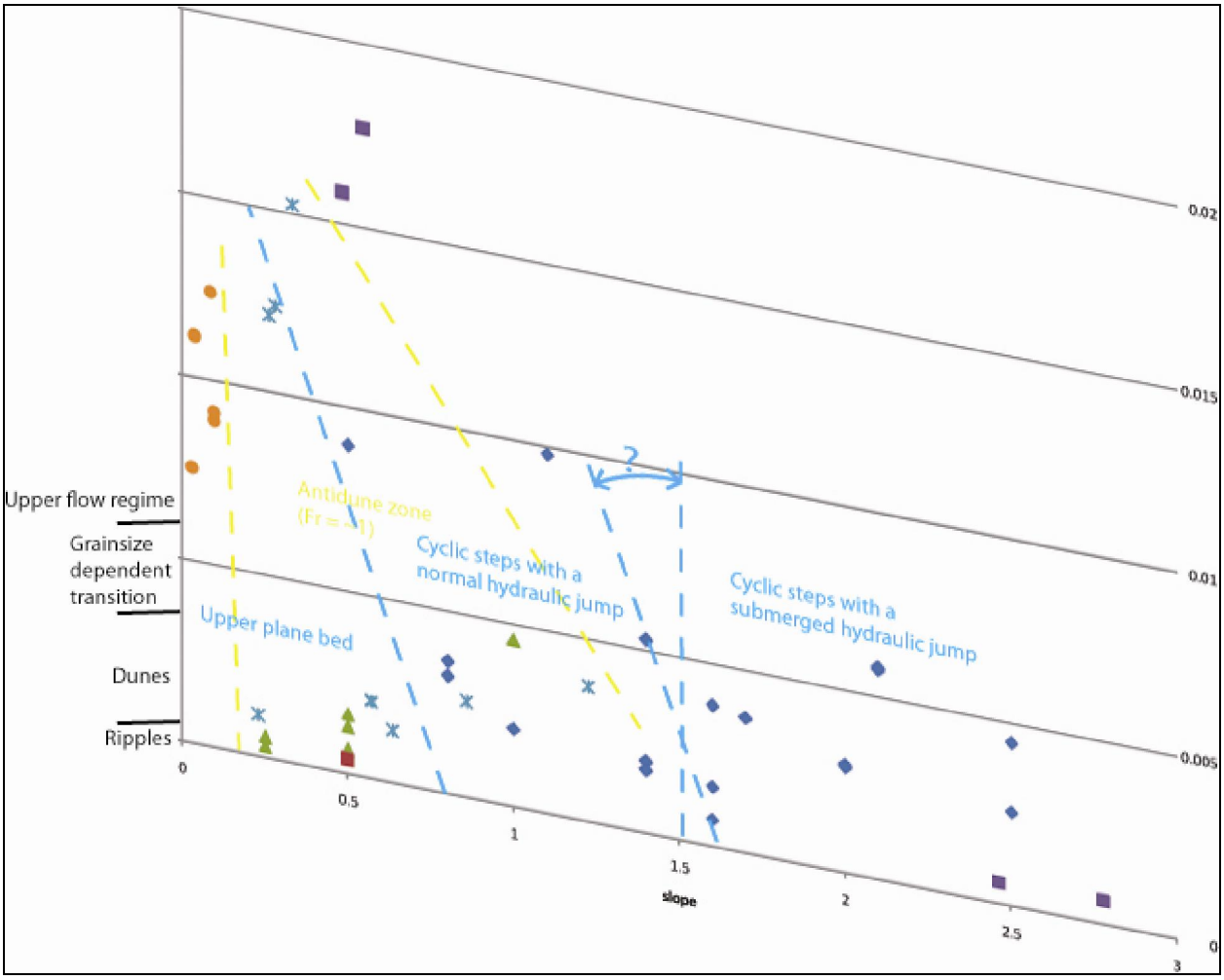

<Figure 5.3, The relation found by Simons and Richardson (1966) for the transition between the lower flow regime bedforms and the upper flow regime are combined with the bedform stability diagram for the upper flow regime of this study and displayed at the left side of the figure. The upper flow regime from Simons and Richardson, for median sediment grain sizes between 0.112 and 0.320 mm start to develop between a streampower of 0.0037 and 0.006. Dunes start to develop for these grainsizes at streampower of 0.0006. The data from Simons and Richardson (1966) has no slope.>

Practical usage

Cyclic steps would only be preserved in the geological record if they are aggradational, migrate laterally, or by channel abandonment. If aggradational cyclic steps are preserved, the sediment inflow would be larger than the outflow, creating a non-stable bedform. This study only covers stable bedforms. Lateral migration might show different settings than tested in this study, because lateral migration often is related to channels with bends. Channel abandonment offers the best situation to be compared with the results from this study.

The streampower could be calculated from cyclic step deposits, using their height (formula 7) or length (formula 8). The state of the hydraulic jump, can be determined if the palaeoslope can be reconstructed. The palaeoslope and streampower values can be used to read the upper flow regime bedform stability graph (figure 4.5) and see whether the state of the hydraulic jump was normal or submerged.

Suggestions for further research

More data from lower and upper flow regimes can be produced to fill in the gabs of the created bedform stability diagram. This study misses a relation for the formation of the cyclic step geometry and the median sediment grain size. This was caused by the absence of equal flow characteristics for different median sediment grain sizes, which is needed to make a comparison. This absence was a result of the flume configuration, where the flow discharge and the regional slope are the variables to set. To test the effect of median sediment grain size on the cyclic step geometry, a configuration is needed where the flow discharge or mixture discharge is the only variable to set.

In this study the variables are the water discharge and the regional slope. The regional slope had to be set, because the used flume configuration desired the formation of a pool with the initial bed used as a natural weir (figure 2.1 f), as described in the methodology. The regional slope is set and a situation where the bedforms are stable ($Sed_{in} = Sed_{out}$) had to be found, by adjusting the sediment feeder. The sediment feeder allows run times as long as there is a sediment supply. With high discharge values run times get very short and might be too short to find stable bedforms. A way to work without a sediment feeder is to use the full width and length of the flume and pump the mixture of water and sediment around. This setting would have one variable, which is the mixture discharge. Also this situation would have complications. Pumping around a mixture of sediment in the used flume would sort the sediment. Sediment would settle out easier in the lower elevated tanks at the up- and downstream ends of the flume, with the coarser particles first. When the pump stops, the finer particles would settle out, resulting in mud drapes, which are hard to erode and alter the flow. This should get a problem when using finer sands with a high mud content. However, when a lot of sediment is used relatively to the available space in the tanks for sediment to settle out, the sorting effect can probably be neglected.

When finer sands are used, the mud content could get a problem when the pump stops. A sediment feeder could help. A pool has to be created at the downstream end of the flume, where the sediment can be collected. The sediment feeder used in this study jams when using wet sediment. The sediment has to be dried first. Sands with a high mud content are almost impossible to dry. For example, I dried a 6 centimeter thick layer of 320 µm sand in an oven at 100 degrees Celsius in 12 hours, while the 120 µm

sands needed more than the double amount of time to dry. Working with dry sand creates clouds of dust, which can cause serious damage to longs. A cap is therefore useful to filter the finer particles out of the air.

Conclusion

- The Froude number on the highest point of a cyclic step reduces when the regional slope increases, as described by formula 2.

- Streampower gives a relation for the cyclic step height (figure 4.1a; formula 7) and cyclic step length (figure 4.1b; formula 8).

- A definition is suggested for spatially periodic bedforms that are delineated by an upstream and downstream hydraulic jump, called chute and pools and cyclic steps in literature. I suggest using the term cyclic steps for the entire class of spatially periodic bedforms, where each wavelength is delineated by an upstream and downstream hydraulic jump, with the additional information of the state of the hydraulic jump, which can be normal or submerged.

- Cyclic steps with a submerged hydraulic jump have a well developed pool, in contrast to cyclic steps with a normal hydraulic jump. A parameter that separates the normal hydraulic jump from the submerged hydraulic jump is the regional bed slope. All normal hydraulic jumps, for median sediment grain sizes between 0.112 and 0.320 millimeter, are formed on a maximum regional slope of 1.4 degrees, while the submerged hydraulic jump is formed with a regional slope with a minimum of 1.7 degrees. This relation can also be seen in the upper flow regime bedform stability diagram using streampower and regional slope (figure 4.5).

- A bedform stability diagram for the upper flow regime is created on streampower versus regional slope, where zones are distinguished for upper plane bed, cyclic steps with a normal hydraulic jump and cyclic steps with a submerged hydraulic jump. Antidunes occur in an overlapping zone with upper plane bed and cyclic steps with a normal hydraulic jump.

- Antidunes are the effect of wave and flow velocity and not from bed characteristics, such as median sediment grain size. Using antidunes in a bedform stability diagram with a flow characteristic other than Froude number results in overlapping zones where the Froude number can be around one.

References

- Alexander, J., Bridge, J.S., Cheel, R.J., Leclair, S.F., 2001. "Bedforms and associated structures formed under supercritical water flows over aggrading sand beds". *Sedimentology 48 (2001), p 133-152.*
- Baas, J., 1991. "Fysische Sedimentologie Deel 1: Regelmatige oppervlaktestroming".
- Boguchwal, L.A. & Southard, J.B., 1990. "Bed configurations in steady unidirectional water flows. Part 3". *Journal of sedimentary petrology, 60, 680-686.*
- Brownlie, W.R., 1981. "Compilation of alluvial channel data: laboratory and field". *Division of Engineering and Applied Science, California.*
- Cartigny,M., Van den Berg, J.H., Mulder, J., Postma, G., 2009. "The mysterious bedforms of the upper flow regime". 33rd *IAHR congress, august 2009.*
- Fagherazzi, S. & Sun, T., 2003. "Numerical simulations of transportational cyclic steps". *Elsevier, Computers & Geosciences 29 (2003) 1143–1154.*
- Fildani, A., Normark, W.R., Kostic, S. & Parker, G. 2006. "Channel formation by flow stripping: large-scale scour features along the Monterey East Channel and their relation to sediment waves". *Sedimentology 53, p. 1265-1287.*
- Fralic, P., 1999. "Paleohydraulics of chute-and-pool structures in a Paleoproterozoic fluvial sandstone". *Sedimentary Geology 125 (1999) 129–134.*
- Garcia, M. & Parker, G., 1989. "Experiments on Hydraulic Jumps in Turbidity Currents near a Canyon-Fan Transition". *Science, New Series, Vol. 245, No. 4916 (Jul. 28, 1989), pp. 393-396.*
- Garcia, M.H., 2008. "Sediment transport and morphodynamics".
- Guy, H.P., Simons, H.P., Richardson, E.V., 1966, "Summary of alluvial channel data from flume experiments, 1956-1961", *US Geological Survey Professional Paper, 1966.*
- Julien, P.Y., Klaassen, G.J., 1995, "Sand-dune geometry of large rivers during floods". *Journal of hydraulic engineering, September 1995, p. 657 – 663.*
- Lamb, M.P., Parsons, J.D., Mullenbach, B.L., Finlayson, D.P., Orange, D.L., Nittrouer, C.A., 2008. "Evidence for superelevation, channel incision, and formation of cyclic steps by turbidity currents in Eel Canyon, California". *Geological Society of America Bulletin, 2008, vol. 120, p. 463-475.*
- Mastbergen, D.R. & Leeuwestein, W., 1986. "Het gedrag van zandmengselstromingen bij zandsluitingen". *Waterbouwkundig Laboratorium, Delft.*

- Mastbergen, D.R., 1987. "Zand-watermengselstromingen". *Waterbouwkundig Laboratorium, Delft.*
- Mastbergen, D.R., 1989. "Zand-watermengselstromingen. Wiskundig model terrasvorming stort". *Report Z299. Delft Hydraulics, Delft.*
- Nemec, W. 1990. "Aspects of sediment movement on steep delt slopes". *International Association of Sedimentologist Special Publication 10, p. 29-73.*
- Parker, G. & Izumi, N. 2000. "Purely erosional cyclic and solitary steps created by flow over a cohesive bed". *Journal of Fluid Mechanics 419, p. 203–238.*
- Shepherd, R.G., 1989. "Correlations of permeability and grain size". *Ground water, vol. 27, No. 5 (1989), p. 633-638.*
- Simons, D.B. & Richardson, E.V., 1966, "Resistance to flow in alluvial channels". *Professional paper 422J, U.S. Geological survey, Washington, D.C.*
- Simons, D.B., Richardson, E.V., Nordin, C.F. 1965. "Sedimentary structures generated by flow in alluvial channels." *Primary Sedimentary Structures and Their Hydrodynamic Interpretation (Ed. G.V. Middleton), SEPM Spec. Publ., 12, p. 34–52.*
- Smith, D.P., Ruiz, G., Kvitek, R., Iampietro, P.J., 2005. "Semiannual patterns of erosion and deposition in upper Monterey Canyon from serial multibeam bathymetry". *Geological Society of America Bulletin, September/October 2005, pp. 1123-1133.*
- Spinewine, B., Sequieros, O.E., Garcia, M.H., Beaubouef, R.T., Sun, T., Savoye, B., Parker, G., 2009. "Experiments on internal deltas created by density currents in submarine minibasins".
- Taki & Parker, 2005. "Transportational cyclic steps created by flow over an erodible bed. Journal of hydraulic research". *Journal of hydraulic engineering, vol. 43, No. 5 (2005), pp 488-501.*
- Van Rhee, C., 2007. "Erosion of granular sediments at high flow velocity". *Hydrotransport 17.*
- Van Rijn, L.C., 1984. "Sediment transport, part III: bed forms and alluvial roughness". *Journal of Hydraulic. Engineering, ASCE, 110(12), 1733-1754.*
- Van Rijn, L.C., 1993. "Principles of sediment transport in rivers, estuaries and coastal seas". *Aqua publications Amsterdam.*
- Vanoni, V.A., 1974. "Factors Determining Bed Forms of Alluvial Streams". *Journal of the Hydraulics Division, Vol. 100, No. 3, March 1974, pp. 363-377.*
- Vanoni, V.A., Brooks, N.H., 1957. "Laboratory studies of the roughness and suspended load of alluvial streams". *California Institute of Technology, No. E-57 (1957).*

- Wynn, R.B., Stow, D.A.V., 2002. “Classification and characterization of deep-water sediment waves”. *Marine Geology 192 (2002), p. 7-22.*
- Winterwerp, J.C., Bakker, W.T., Mastbergen, D.C., Van Rossum, H, 1992. “Hyperconcentrated Sand-Water Mixture Flows over Erodible Bed*”. Journal of Hydraulic Engineering, Vol. 118, No. 11, November 1992, pp. 1508-1525.*
- Yang, C.T., Stall, J.B., 1974. “Unit Stream Power for Sediment Transport in Alluvial Rivers”. *Research Rep 88.*